

The S_{B9} catalogue^{*}: status, comparison with non-single stars from *Gaia* DR3 and evolution to S_{Bx}

T. Merle^{1,2,†}, A. Jorissen¹, S. Alexandre¹, J. Desuter¹, C. Loup³, A. Tokovinin⁴, G. Travençolo⁵, M. Van der Swaelmen⁶, S. Van Eck¹, G. Van de Steene², J. Southworth⁷, and G. Sadowski¹

¹ *BLU-ULB, Institut d'Astronomie et d'Astrophysique, Université Libre de Bruxelles, 1050 Brussels, Belgium*

² *Royal Observatory of Belgium, Avenue Circulaire 3, 1180 Brussels, Belgium*

³ *Observatoire astronomique de Strasbourg, CDS, Université de Strasbourg, CNRS, UMR 7550, Strasbourg, France*

⁴ *Cerro Tololo Inter-American Observatory, NSF's NOIRLab Casilla 603, La Serena, Chile*

⁵ *Faculty of Mathematics & Physics, University of Ljubljana, Jadranska 19, 1000 Ljubljana, Slovenia*

⁶ *INAF - Osservatorio Astrofisico di Arcetri, 50125, Firenze, Italy*

⁷ *Astrophysics Group, Keele University, Keele, Staffordshire ST5 5BG, UK*

Accepted XXX. Received YYY; in original form ZZZ

ABSTRACT

The Ninth Catalogue of Spectroscopic Binary Orbits (S_{B9}) is a comprehensive compilation of spectroscopic binaries (SBs) with orbital parameters sourced from the literature, comprising approximately 4000 systems with about 2800 single-lined and 1200 double-lined binaries. This work presents the latest status of the S_{B9} catalogue after over two decades of development since its online inception in 2004. In particular, we expose the statistical properties of SBs in terms of orbital period distributions and eccentricity-period diagrams per spectral type and evolutionary stage. We perform a careful cross-match with the *Gaia* Data Release 3 (DR3) to update astrometric parameters and compare with the *Gaia* DR3 Non-Single Star (NSS) catalogue. Our cross-matching approach uses positional separations, magnitudes, and proper-motion back-propagation to identify counterparts. The final S_{B9} version updated by D. Pourbaix (2021-03-02) includes 4003 SB systems, some in higher-order multiples: 152 in triples, 71 in quadruples and 14 in higher-order systems. Among these 4003 SB, 3976 have matching *Gaia* DR3 identifiers, while 21 are too bright and six too faint for *Gaia* detection. red Ten S_{B9} systems with periods larger than 1180 d (including a spectroscopic triple) have been spatially resolved by *Gaia* DR3. We identify a common sample of 827 S_{B9} binaries cross-matched with *Gaia* NSS, among which 655 are considered as reliable, based on relative period and absolute eccentricity differences not exceeding 10%. The limited overlap (21% of S_{B9}) is primarily due to selection cuts in NSS SB1 analysis, brightness limits, temporal baselines, and partial orbital solutions in the *Gaia* NSS catalogue. This study highlights the strengths and limitations of both catalogues and establishes a clean benchmark sample for future binary star research. Our work marks the transition of S_{B9} into S_{Bx} , *The eXtended Catalogue of Spectroscopic Binary Orbits*^{*}, featuring a modern relational database, improved web interface, and Virtual Observatory access standards, aiming to enhance accessibility, data quality, and analysis capabilities for the binary and multiple star community.

Key words: (stars:) binaries: spectroscopic – (stars:) binaries (including multiple): close – techniques: spectroscopic – techniques: radial velocities – catalogues

1 INTRODUCTION

Spectroscopic binaries (SB) are nowadays routinely detected in every large spectroscopic survey, by measuring radial-velocity (RV) variations either in temporal series of one visible component (SB1) or between two (or more) visible components (SB n , with $n \geq 2$). Although detection is relatively easy, orbital characterisation requires a good sampling along the orbital cycle, which is only reachable for a marginal fraction of large spectroscopic-survey targets. For instance, there were only two SB1 (among 800 detected) for which we could determine an orbital solution from the observations obtained by the

Gaia-ESO Survey (Merle et al. 2020). In the infrared APOGEE survey DR16 and DR17, about 8 000 SB candidates were identified, out of which a bit more than 300 have enough observations to constrain the orbital parameters (Kounkel et al. 2021). With the advent of the detection of dormant black holes in SB1 (with an early-type primary by Mahy et al. 2022; Shenar et al. 2022, and now even around late-type stars by El-Badry et al. 2023; Gaia Collaboration 2024), it is of the uttermost importance to have a database of SB with reliable orbital and astrophysical parameters.

The *Ninth Catalogue of Spectroscopic Binary Orbits* (S_{B9} , Pourbaix et al. 2004) is an historical compilation of spectroscopic binaries with orbital parameters. It is the online continuation of the printed catalogue SB8 (Batten et al. 1989) which contains 1 469

^{*} <https://www.astro.ulb.ac.be/sbx>

[†] E-mail: thibault.merle@ulb.be

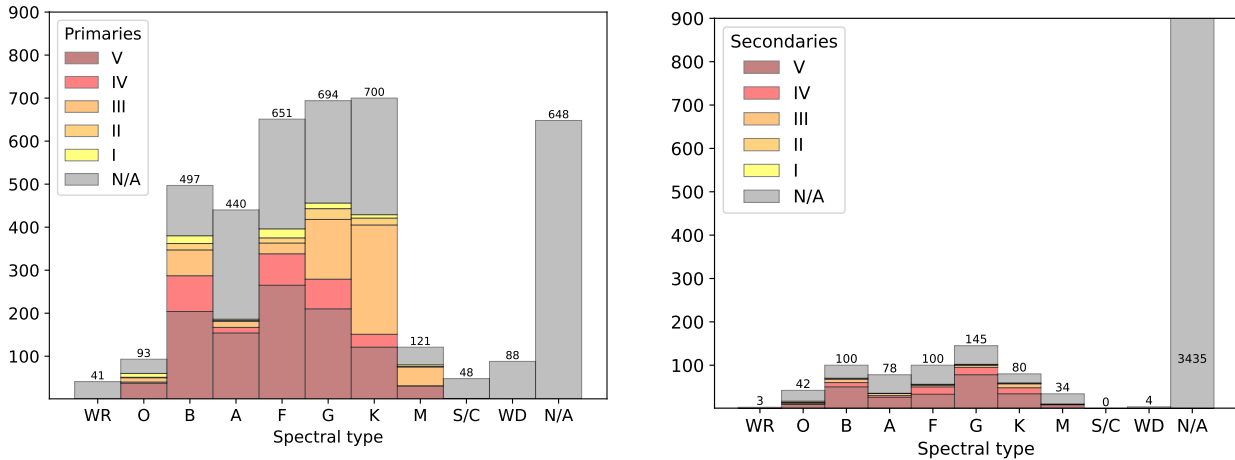


Figure 1. Distribution of the S_{B9} binaries per spectral type and luminosity class for primaries (left) and secondaries (right). There are 16% of primaries without spectral type (grey in the left panel) and only 9% of secondaries with a spectral type (non-grey in the right panel).

SB systems and critical notes on most of the systems¹. For completeness we recall the earlier versions of this catalogue, historically started at the Lick Observatory, with the five first versions of the SB catalogue (Campbell & Curtis 1905; Campbell 1910; Moore 1924, 1936; Moore & Neubauer 1948); then pursued at the Dominion Astrophysical Observatory with the sixth (Batten 1967), seventh (Batten et al. 1978) and eighth (Batten et al. 1989) versions of the catalogue. Since 2000, and under the advocacy of A. Tokovinin, the catalogue was sponsored by the IAU, through the former commission C30 (‘Radial Velocities’) inherited by commission G1 (‘Binary and Multiple Star Systems’) in 2015, led by D. Pourbaix² and hosted at the *Université Libre de Bruxelles*, Belgium. The last update of the S_{B9} catalogue by D. Pourbaix was done on 2021-03-02, and contains more than 5 000 orbits. The queryable database is available at <https://sb9.astro.ulb.ac.be/> with a mirror at CDS Vizier <https://cdsarc.cds.unistra.fr/viz-bin/cat/B/sb9>. We stress that this version was the last maintained by D. Pourbaix and does not include the recently revised orbits using HERMES/Mercator (Raskin et al. 2011) spectroscopic data for about 50 systems (Merle et al. 2024), and about 56 spectroscopic orbits, many belonging to stellar triples from Tokovinin & Latham (2020) and Tokovinin (2020, 2022).

The S_{B9} catalogue serves as a reference and comparison sample for numerous studies on stellar binaries. It is also highly valuable due to its copious notes. We try to compile here a non-exhaustive list of most important studies which are based on the S_{B9} catalogue. It has been of fundamental importance for reviews on stellar multiplicity (e.g. Duchêne & Kraus 2013; Moe & Di Stefano 2017) and other disciplines like astroinformatics (Abushattal et al. 2022). It was also used in large spectroscopic surveys (e.g., Gaia-ESO: Merle et al. 2020, APOGEE: Kounkel et al. 2021, LAMOST: Li et al. 2025). The S_{B9} catalogue can be used as well for selecting samples for astrometric studies (e.g. Jancart et al. 2005; Frankowski et al. 2007; Belokurov et al. 2020) and for feeding other databases (e.g. MSC: Tokovinin 2018). It can serve for searching for companions to close SBs (Tokovinin et al. 2006), investigating solar-like oscillators (Beck

et al. 2024), or solar twins (Simon & Obbie 2009), and studying stellar rotation in B-type stars (Huang et al. 2010), etc. It can serve as a reference for testing new techniques like Bayesian inference or Markov Chain Monte Carlo methods (e.g. Videla et al. 2022; Anguita-Aguero et al. 2022; Leclerc et al. 2023). It is also important for understanding the impact of the companions on the evolution of stars (e.g. Mazeh 2008; Eggleton & Tokovinin 2008), for searching for brown-dwarf companions (Sahlmann et al. 2011), or compact companions (Jayasinghe et al. 2023), and even in exoplanetary science (Winn & Fabrycky 2015).

The *Gaia* mission (Gaia Collaboration 2016) is an ambitious ESA spacecraft measuring the positions, parallaxes, proper motions and magnitudes of about 2 billion stars. In addition the on-board Radial Velocity Spectrometer (RVS, Katz et al. 2023) provides RV for more than 33 millions stars. The third Data Release (DR3, Gaia Collaboration 2023a) includes the Non-Single Star catalogue (NSS, Gaia Collaboration 2023b) which outclasses, in a single release, all the binary catalogues known so far. In summary, the NSS catalogue includes 813 000 sources, and among them about 277 000 SB. The individual epoch spectra will be released in DR4.

The goal of the present work is to present the status of the last version of the S_{B9} catalogue (Sect. 2), to present its careful cross-match with *Gaia* DR3 (Sect. 3), and to critically compare it with the *Gaia* DR3 NSS catalogue (Sect. 4). Finally we discuss the long-term future improvements planned for the S_{B9} database (Sect. 5).

2 CURRENT STATUS

2.1 SB1 and SB2

In the S_{B9} catalogue, each entry is identified by a *system number* to which several orbits may be attached. A unique *orbit number* is associated to the corresponding published reference. In the current version (2021-03-02), there are exactly 5042 orbits belonging to 4021 binaries (i.e. S_{B9} systems). We immediately note that some of these S_{B9} systems can be part of higher-order stellar multiples, preventing us, at present, from clearly stating how many physical stellar multiples there are in the S_{B9} catalogue. To identify SB1 and SB2, we look at

¹ Available on CDS Vizier at <https://cdsarc.cds.unistra.fr/viz-bin/cat/V/64>

² who deceased on Nov. 14, 2021

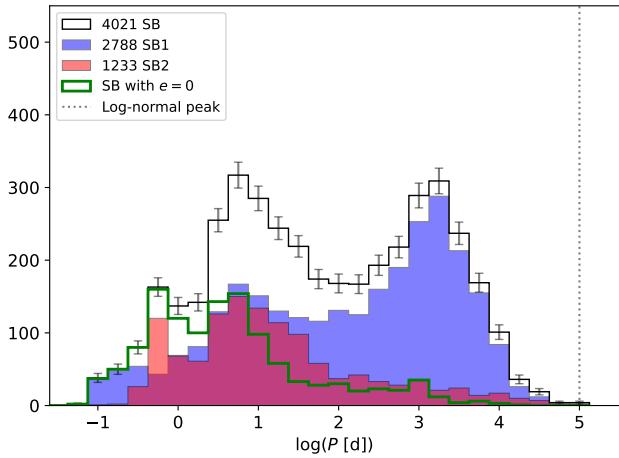


Figure 2. Distribution of the orbital periods of the SB1, SB2 and combination of them. The distribution shows three peaks at 0.6, 7 and 1800 d which are discussed in the text. **Error bars are taken as Poissonian.** The dotted line represents the mode of the log-normal distribution of binaries (Moe & Di Stefano 2017) peaking around 270 a. SBs lie on the short-period side of this distribution.

orbits that have non-null semi-amplitudes K_1 or K_2 ³ (SB1), or K_1 and K_2 (SB2), respectively. It should be noted that there are 129 S_{B9} systems which have both SB1 and SB2 orbital solutions. We consider them as SB2 in the subsequent analysis, since their composite nature has been revealed. In the S_{B9} catalogue, 2/3 of the system numbers are SB1 (2788) and 1/3 are SB2 (1233). RV data are included in the catalogue for 3 111 S_{B9} systems representing 77% of all systems. Systems with missing RV data come from earlier versions of the catalogue, and a quick look at some of these systems reveals that these data are generally available in the original publications, but not easy to extract. Finally, a grade from 0 (tentative) to 5 (definitive)⁴ was originally set for each orbit but was gradually abandoned in the last version of the catalogue. In fact, the grading scheme was not based in any way on objective criteria but was based on the subjective experience of the providers of the earliest versions. D. Pourbaix had started to think about a new grading scheme, but this scheme was never implemented. About half of the orbits have a grading mark.

2.2 Statistical properties

2.2.1 Spectral types and luminosity classes

The S_{B9} catalogue lacks a quantitative astrophysical characterisation of the stars. The components of each SB are only characterised by a spectral type and a luminosity class, when available. The spectral type classification generally comes from the M-K scheme reported by the authors who published the orbital parameters, except for 145 SBs with A-F primaries (from Abt 2009). The distribution per spectral type and luminosity class of the S_{B9} primaries and secondaries are displayed on Fig. 1. Neither the distribution of stars among spectral types nor the distribution of luminosity classes do reflect the stellar mass function. In the S_{B9} catalogue, SBs with an early-type primary are over-represented while late-type dwarf primaries are

under-represented as compared to giants. For GKM spectral types, main-sequence (V) stars are also largely under-represented. We stress that the fraction of primaries without a determined spectral type (16%) or a luminosity class (51%) is fairly large, increasing to 85% and 91% for secondaries, partially explained by the fact that there are approximately 2/3 of SB1 and 1/3 of SB2 in the S_{B9} catalogue. The fraction of SB2 with a known spectral type or luminosity class is 46% and 30% respectively. This situation calls for improvements (see Sect. 5).

2.2.2 The orbital-period distribution

The aggregated orbital-period distribution (black line) for all SBs in the S_{B9} catalogue is presented in Fig. 2. In addition, we show the distributions for SB1s (blue shading), SB2s (red shading), and circular SBs (green line). Almost all SBs with periods shorter than 1 d have been circularised. The aggregated orbital-period distribution presents three peaks at ~ 0.6 , ~ 7 and 1800 d. Interpreting the characteristics of these distributions is challenging, as their properties emerge from multifaceted origins, encompassing both physical mechanisms and selection biases. In the following, we try to disentangle these influences.

We show on the left panel of Fig. 3 SBs with dwarf primaries and on the right SBs with giant primaries colour-coded per spectral type. We also added the theoretical expectations for the minimum period for a given spectral type assuming equal-mass contact binaries on the main sequence, *i.e.*, with the primary filling its Roche lobe. We use the formula from Eggleton (1983) to express the Roche radius R_{\max} . From Kepler’s third law, it is then possible to evaluate the minimum period P_{\min} of a binary system able to host a Roche-lobe-filling star ($R_{\max} = R$) of a given spectral type characterized by radius R and mass M :

$$P_{\min} = 0.35 R_{\max}^{3/2} M^{-1/2} \quad (1)$$

with P_{\min} in days, and M and R_{\max} in solar units. We use an updated version of the calibrations of Pecaut & Mamajek (2013) for estimating M and R_{\max} per spectral type. For clarity, we show individual panels per spectral type in Appendix A (Fig. A1). We now try to decode the shape of the orbital-period distribution with a mixture of physical and observational-bias effects.

The left-hand ridge of the first peak (around 0.6 d) is clearly associated with the physical limit of contact-binary orbits as demonstrated by the left panels of Figs. 3 and A1. The theoretical minimum-period expectations for contact binaries go from 0.1 d for M dwarfs to 1 d for O dwarfs which are well matched by the observed distributions, except for M dwarfs. The latter are much less numerous than the other spectral types in S_{B9} despite constituting the vast majority of stars. The SB with the shortest orbit in the S_{B9} catalogue is an SB1 cataclysmic variable: the dwarf nova GW Lib with an orbital period of 1.280 ± 0.001 h (Thorstensen et al. 2002). On the contrary, the right-hand shallower slope of the first peak is probably an observational bias caused by (i) astronomers favouring studies of contact binaries (hence the number of contact binaries with a derived orbit is larger than their longer-period neighbours), and (ii) orbits of early-type binaries, with their few broad lines, are increasingly difficult to characterize at large periods when the RV amplitude becomes small.

The second peak (around 7 d) is, like the first peak, probably a combination of observational and physical effects. Even though this second peak corresponds to the maximum of the orbital-period distribution of SB2 systems (*i.e.*, with nearly twin components), a look at Fig. A1 showing the distribution of SB2 systems among the

³ There are 11 orbits for which K_2 alone is defined.

⁴ A unique system has a grade of 5.1, it is S_{B9} system 815, *i.e.* α Cen.

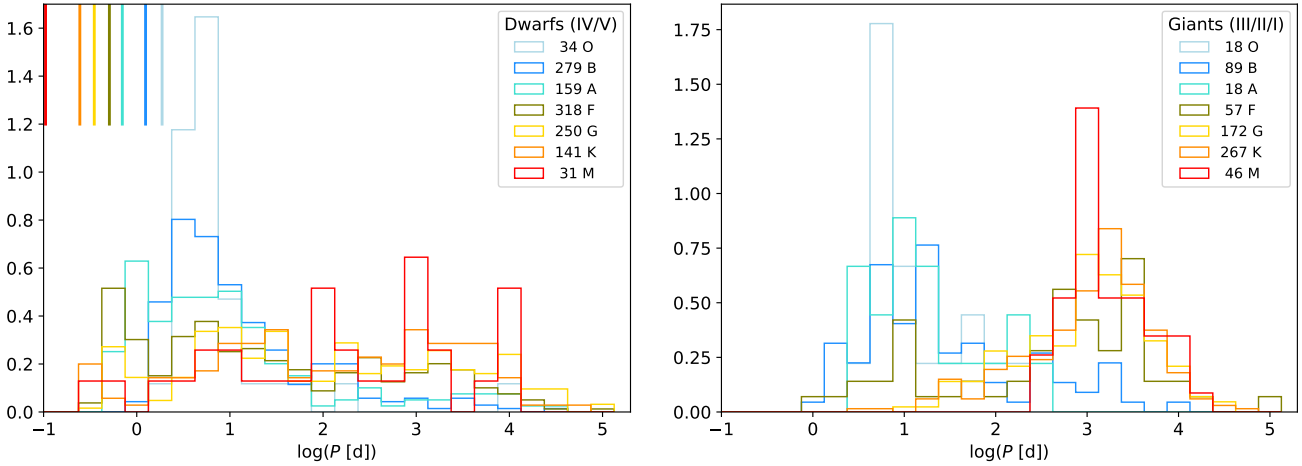


Figure 3. Distribution of the orbital periods per spectral type for dwarfs (left) and giants (right) of SB primary components. The y-axis corresponds to the period distribution normalised so that the integral of the frequency times the bin size equals unity. Colour codes the spectral types. In the left panel, vertical lines correspond to the minimum period for a given spectral-type from contact equal-mass binaries.

different dwarf spectral types reveals that this correspondence seems to be purely coincidental with no background physical meaning.

The origin of the second peak is more difficult to trace than the first peak. On its left ridge, the peak probably results from the early-type-star (O and B) period distribution peaking at about 7 d (close to their contact limit below which the period distribution cannot go) with the later types presenting a dip at periods slightly shorter than 7 d, before climbing up again towards their contact threshold (Fig. A1). On its right ridge, the peak at 7 d seems to be the combination of the number of early-type orbits diminishing towards longer periods (as already argued in relation with the first peak, since for O-type stars, the first and second peaks are superimposed) and the period distribution of late-type stars remaining flat. The above arguments alone would hint at the biased nature of the 7 d peak. However, several physical scenarios have been developed to explain the accumulation of binaries in the period range from 1 to 10 d (Merle 2024, and references therein). Among them, secular evolution through Kozai-Lidov cycles and tidal friction involving a third distant companion (*i.e.* evolution of compact hierarchical triples) is appealing (*e.g.* Fabrycky & Tremaine 2007; Bataille et al. 2018; Libert 2022, see also Fig. 25 in Gosset et al. 2025). This scenario is also supported by the stellar triples recently found by comparing *Gaia* NSS astrometric acceleration and SB solutions (Gaia Collaboration 2023b), and the ones found by cross-matching with the catalogue of wide binaries (El-Badry et al. 2021), which all show a peak between 5 and 10 d (see Figs. 52, 53, and 54 in Gaia Collaboration 2023b). Binaries with late-type (G, K, M) giant primaries (right panels of Figs. 3 and A1) do not contribute to the second peak, since the physical limit set by the Roche-lobe radius makes P_{\min} increase along the red and asymptotic giant branches.

The third peak at ~ 1800 d (5 a) is dominated by SB1 involving a late-type primary. It is clearly an observational bias because, for periods beyond this peak, the RV variations drop below the detection limit of current spectrographs, while orbital periods of the widest bound pairs may reach $10^8 - 10^9$ d (*e.g.*, Proxima Cen orbits α Cen in approximately half a million years; see, *e.g.*, Kervella et al. 2017). For SB1s in *Gaia* DR3 NSS, this peak is just below 1000 d and only reflects the inability of *Gaia* DR3 to detect binaries with an orbital period much longer than the RV-monitoring time span (3 years for

Gaia DR3). It is indeed clear from studies gathering all kinds of binaries (thus including visual binaries – VB) that the main reservoir of binaries (*i.e.* at the peak of the log-normal distribution) is located around 230 a (Moe & Di Stefano 2017). The SB with the longest period in the S_{B9} catalogue is a twin VB-SB2 of K0V components with an estimated period of 320 ± 20 a (Pourbaix 2000), which is close to the peak position of the log-normal distribution of late-type stars (Moe & Di Stefano 2017). Therefore, the lack of long-period SBs is primarily due to the absence of long-term RV data series. Such data are available only for a modest number of relatively bright stars, and their uncertainties often exceed a few km s^{-1} .

2.2.3 The eccentricity-period diagram

The eccentricity-period diagram for the S_{B9} catalogue is displayed in Fig. 4 for dwarf primaries (left) and giant primaries (right) colour-coded by spectral type. Since models predict that binaries can form at all eccentricities (except may be at the smallest ones: $e \leq 0.05$), the presence of an upper envelope to the data points may be interpreted as the signature of the tidal processes leading to the many circular orbits accumulating at the shortest periods, and depleting in priority the upper left corner of the eccentricity-period diagram. Circularisation mechanisms are still highly debated, and the corresponding theoretical and observed behaviour is best illustrated in Barker (2022) and Mirouh et al. (2023). In Fig. 4, we show the *empirical* envelope $e_{\max} = 1 - (P_0/P)^{1/3}$ fitted by Pourbaix et al. (2004) on S_{B9} data with the circular period $P_0 = 0.35$ d roughly corresponding to contact systems of solar-type stars (Table 1). Comparing the left and right panels of Fig. 4, we notice a shift of the envelopes towards longer periods with later spectral types, much better marked for giants as compared to dwarfs. This shift has not the same origin for dwarf and giant primaries though, as we now discuss. For clarity, we show individual panels (for dwarf and giant primaries per spectral type) in Appendix A, Fig. A2. There we used instead the *periastron* envelope⁵ $e_{\max} = 1 - (P_c/P)^{2/3}$ derived from the Roche lobe theory (Mazeh

⁵ For the sake of completeness, we also mention the existence of the *circularisation* envelope $e_{\max} = [1 - (P_c/P)^{2/3}]^{1/2}$ derived from equilibrium-tide theory (Hut 1981) that we do not use in the present work.

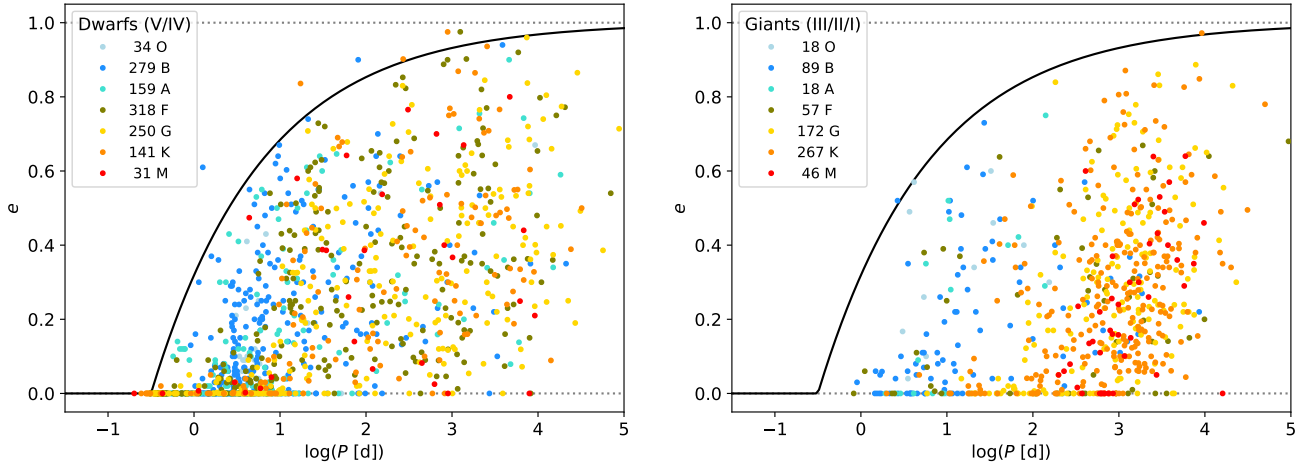


Figure 4. The $e - \log P$ diagram of the S_{B9} binaries colour-coded by spectral type for dwarfs (left) and for giants (right panel). The solid line is the *empirical* fit to the S_{B9} data (Pourbaix et al. 2004).

Table 1. Circular periods P_c as a function of the filling factor f for a typical giant primary of $2 M_{\odot}$ and for typical main sequence primaries. Components of equal masses have been assumed.

Spectral Type	M [M_{\odot}]	R [R_{\odot}]	P_c [d]		
			$f = 1.0$	$f = 0.5$	$f = 0.25$
Giants					
	2.0	500	2800	7800	22000
	2.0	100	250	700	2000
	2.0	10	7.8	22	63
Dwarfs					
O	35	10	1.9	5.3	15.0
B	9.9	5.0	1.2	3.5	10.0
A	2.0	2.0	0.7	2.0	5.6
F	1.3	1.4	0.5	1.4	4.1
G	1.0	1.0	0.4	1.0	2.8
K	0.7	0.7	0.2	0.7	2.0
M	0.3	0.3	0.1	0.3	0.8

2008; Jorissen et al. 2009). We may generalise Eq. 1 by introducing the filling factor $f = R/R_{\max}$:

$$P_c = 0.35(R/f)^{3/2}M^{-1/2}, \quad (2)$$

thus defining a critical period for circularisation in systems which reach a filling factor f at periastron, with P_c in days and M and R_{\max} in solar units. Typical values per spectral type are provided in Table 1 together with circular periods for the three filling factor values of 1, 0.5 and 0.25, displayed on the left panels of Fig. A2.

For systems with late-type dwarf primaries (left panels of Figs. 4 and A2), the absence of eccentric systems in the $e - \log P$ diagram at short periods does not result from an observational bias, but rather is an evolutionary effect, as we now explain. In Fig. A2, we first draw the periastron envelope corresponding to the circular period for a filling factor of 1 (Table 1 and solid line in Fig. A2), which is similar to the period threshold for contact systems. There are thus very few systems falling to the left of this envelope. Then we draw with dashed and dotted lines the envelopes corresponding to filling factors of 0.5 and 0.25, respectively. It clearly appears that the region enclosed by the $f = 0.25$ and $f = 1$ envelopes are less populated as one considers

later spectral types. This results from the fact that, because late-type stars live longer, they have more time to circularise, and hence, circularisation may involve systems with smaller filling factors where tides (and thus circularisation) are less efficient and circularisation thus takes longer (see, e.g., Meibom & Mathieu 2005).

For systems with giant primaries (right panels of Figs. 4 and A2), the increase from a few days to hundreds of days in the circularisation period is related to the increasingly large radii associated with giants of later spectral types since the radius increases as the stars evolve along the giant branch, ending up as very large asymptotic-giant-branch stars of late M types – besides our Figs. 4 and A2, this has been illustrated as well in Figs. 24 and 25 of Gaia Collaboration (2023b). Early-giant primaries are of similar size as their dwarf counterparts, which is why they have a similar circularisation period (a few days) as dwarfs. In contrast, late-giant primaries can reach hundreds of solar radii and imply a circularisation period of two orders of magnitude larger than that of dwarf primaries.

3 CROSS-MATCH WITH *Gaia* DR3

We performed a cross-match of the S_{B9} catalogue with *Gaia* DR3 (Gaia Collaboration 2016, 2023a). Cross-matching catalogues is a complex and challenging problem, because there are no general rules to determine whether two observations made with different telescopes, at different wavelengths, with different resolutions, and at different epochs, are physically related to the same target. In other words, looking only at the closest separations is not always a guarantee to get the proper match. Different approaches exist: for instance using positions, position uncertainties and proper motions is an option, see, e.g. the cross-matched catalogues of *Gaia* DR1 and DR2 with external catalogues like 2MASS, ALLWISE, HIPPARCOS, etc. (Marrese et al. 2017, 2019). They promote homogeneity and consistency and avoid the use of *a priori* knowledge based on photometry for instance. Nevertheless, including proper motions does not address the astrometric-binary problem (the disturbance introduced by the orbital motion on the proper motion) as it would be necessary to include the binary orbits when available. Other approaches use combinations of requirements based on photometry and radial velocity (e.g. Tsantaki et al. 2022). A cross-match process is always a

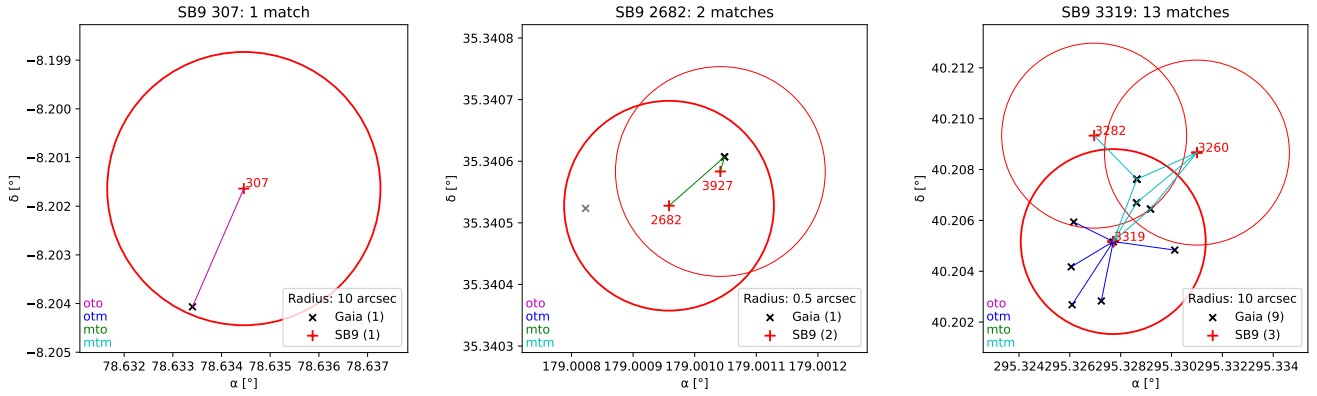


Figure 5. *Left:* one-to-one cross-match for the S_{B9} system 307 (β Ori B, $G = 6.6$). β Ori A is too bright to be observed by *Gaia*. The S_{B9} system 307 was wrongly assigned the coordinates of β Ori A (in S_{B9}) explaining such a large separation in the match. This example illustrates the need to have a large cone search radius value of 10 arcsec. *Middle:* zoom on many-to-one matches for the S_{B9} systems 2682 and 3927 separated by 0.14 arcsec, not resolvable by *Gaia*. For readability, the radius in the plot has been decreased to 0.5 arcsec. The grey cross corresponds to the *Gaia* source at epoch J2016.0. *Right:* one-to-many and many-to-many cross-matches for the S_{B9} system 3319 (TIC 139154020, $G = 15.7$), member of the open cluster NGC 6819. This cross-match involves two other S_{B9} systems and three *Gaia* DR3 sources leading to six one-to-many and three many-to-many matches.

compromise between the number of requirements and the fraction of mismatching objects. Here we aim at minimising this fraction.

Within S_{B9} , *Gaia* DR2 and DR3 identifiers were already implemented by D. Pourbaix, but unfortunately, we did not have access to the methodology of his assignments. That is why we decided to make our own cross-match, and compare them with Pourbaix’s and SIMBAD classification. ‘SIMBAD focuses on the objects of interest’⁶ and at the time of the starting of this project, not all S_{B9} systems were added to it. The cross-identification between the SIMBAD database and *Gaia* DR3 has been performed in May 2022, involving 6.5 millions of objects, excluding objects with coordinates less precise than the sub-arcsecond level (quality D and E).

Before cross-matching, we uploaded the S_{B9} catalogue to the *Gaia* archive, selected systems using ADQL queries, and performed an epoch back-propagation to account for proper motion, resulting in 3981 matched systems out of 4021, while identifying 21 overly bright (Table 2) and six overly faint systems (Table 3) not present in *Gaia* DR3. The details of the adopted strategy is given in Appendix B. We describe in the following section the workflow to determine the best matches.

3.1 Different types of resulting matches

Ideally, we should obtain one *Gaia* target match per S_{B9} system (one-to-one). But within a cone search of 10 arcsec, centred on each S_{B9} system, several matches with the dense *Gaia* catalogue may occur (one-to-many). Conversely, less often, several S_{B9} systems can match a unique *Gaia* source (many-to-one). In some additional cases, several S_{B9} systems (closer than 20 arcsec from each other) can match similar *Gaia* targets (many-to-many). We may summarise the matches in these four categories as follows:

- 2068 one-to-one (*oto*) matches for 2068 S_{B9} systems;
- 6327 one-to-many (*otm*) matches for 1651 systems; the maximum number of matches for one S_{B9} system is 50, this system being in the bulge (S_{B9} 2452).

- 141 many-to-one (*mto*) matches for 141 systems; the maximum number of S_{B9} identifiers for one *Gaia* source is 4.
- 504 many-to-many (*mtm*) matches for 144 systems.

Note that 23 S_{B9} systems fall both in the *otm* and *mtm* matching categories. Illustrating examples are provided in Fig. 5 showing how complicated the cross-matches can be: on the left panel, the ideal case of *oto* match (in magenta) between S_{B9} and *Gaia*; on the middle panel, the *mto* case (in green) where two S_{B9} systems match the same *Gaia* source, in that case corresponding to a spectroscopic triple unresolved by *Gaia*; and on the right a complicated case combining *otm* and *mtm* where several *Gaia* sources match the S_{B9} system (*otm*, in blue) while other *Gaia* sources also match several other S_{B9} systems (*mtm*, in cyan).

3.2 Filtering the cross-matches

3.2.1 Euclidean distance

For each S_{B9} system, we use an Euclidean distance on angular separation ρ and difference of G -band magnitudes ΔG of the matches to automatically select the one with minimum d , where:

$$d = \sqrt{\left(\frac{\rho}{\langle\rho\rangle}\right)^2 + \left(\frac{\Delta G}{\langle\Delta G\rangle}\right)^2} \quad (3)$$

with $\langle\rho\rangle = 0.06$ arcsec and $\langle\Delta G\rangle = 0.04$ are the median angular separation and magnitude differences of all the matches at J2000.0 in a cone search radius restricted to one arcsec. Nevertheless the magnitudes provided in the S_{B9} catalogue are not the G magnitudes of *Gaia*. Transformation to the *Gaia* G magnitude thus needs to be done, as we describe in the next section.

3.2.2 Transformation from S_{B9} to *Gaia* magnitudes

In the S_{B9} catalogue, an integrated magnitude is given with its associated filter. It is mainly given in V band (89%), but 6% of systems have no magnitudes, 2% have B magnitudes, 1% have ‘ P ’ magnitudes, meaning ‘Photographic’ historically coming from SB8 (Batten

⁶ <http://simbad.cds.unistra.fr/guide/catalogues.htm>

Table 2. The 21 brightest S_{B9} systems without any match in *Gaia* DR3, ordered by decreasing brightness.

V [mag]	S_{B9}	Type	Bayer name	Common name	HIP	Remark
-1.46	416	SB1	α CMa	Sirius	32349	Brightest star, with a WD companion
-0.10	815 ¹	SB2	α Cen	Rigel Kentaurus & Toliman	71683 71681	Resolved components (16.5 arcsec) with distant companion Proxima Cen
0.08	306	SB1	α Aur	Capella	24608	Brightest subsystem of a stellar 2+2 quadruplet ²
0.37	467 ¹	SB1	α CMi	Procyon	37279	WD companion
0.97	766	SB2	α Vir	Spica	65474	β Cep variable; innermost subsystem of 3+1 quadruplet ²
1.25	2446	SB1	β Cru	Mimosa	62434	Upper Sco–Cen association
1.33 ³	725	SB1	α Cru	Acrux	60718	Brightest subsystem of a stellar 3+3 sextuplet ²
1.79	648	SB1	α UMa	Dubhe	54061	Resolved (0.7 arcsec) subsystem of 3+2 quintuplet ²
1.83	500	SB2	γ^2 Vel	Regor	39953	Wolf–Rayet
1.90	366	SB2	β Aur	Menkalinan	28360	
1.90	462	SB1	α Gem A	Castor A	36850 A	Forms a quadruple with Castor B at 3 arcsec
1.92	410	SB1	γ Gem	Alhena	31681	
1.92	1234	SB1	α Pav	Peacock	100751	Tucana Horologium association
2.02	76	SB1	α UMi	Polaris	11767	Cepheid variable, innermost subsystem of a triplet ²
2.06	4	SB2	α And/ δ Peg ⁴	Alpheratz/Sirrah	677	RS CVn-type variable, resolved (24 mas) binary with companion at 6.7 arcsec ²
2.22	158	SB2	β Per	Algol	14576AB	Outer pair (0.1 arcsec; 680 d)
2.25	157	SB2	β Per	Algol	14576A	Inner pair (2.3 mas) eclipsing binary of 2.8 d
2.32	1837	SB1	δ Sco	Dschubba	78401	Upper Sco association
2.55	793	SB2	ζ Cen		68002	
2.65	98	SB2	β Ari	Sheratan	8903	
3.00	461	SB1	α Gem B	Castor B	36850 B	Forms a quadruple with Castor A at 3 arcsec

Notes. Apparent V magnitudes come from SIMBAD unless specified. The type distinguishes whether the system has been identified as SB1 or SB2 in S_{B9} .

¹ Rejected as best match with unrelated *Gaia* source.

² From the Multiple Star Catalogue (Tokovinin 2018).

³ Magnitude from Hoffleit & Warren (1995).

⁴ This system belongs to two constellations.

Table 3. The six S_{B9} systems without any match in *Gaia* DR3 because they are too faint in G . All are SB1.

V [mag]	S_{B9}	Name	Remark
17.5 ¹	2469	SDSS J022502.06+001541.0 ³	Period of 3.6 d
22.5	1137	PSR J1915+1606	Hulse–Taylor pulsar, period 0.32 d
22.8	2467	SDSS J005406.06+003432.0	Period of 15.9 d
>23 ⁵	480	UY Vol	Low-mass X-ray binary, period 0.15 d
23.3 ²	511	PSR J0823+0159	Pulsar, period 1710 d
26.9 ⁴	1421	PSR J2305+4707	NS+WD binary, $P = 12.3$ d, $e = 0.66$

Notes. Apparent magnitudes are taken from SIMBAD unless otherwise specified.

¹ Magnitude in r band from S_{B9} .

² Magnitude in r band from SIMBAD.

³ Only two identifiers in SIMBAD, from SDSS and S_{B9} .

⁴ From van Kerkwijk & Kulkarni (1999).

⁵ Quiescent V magnitude from Tan et al. (1992); $V = 16.9$ reported by SIMBAD.

et al. 1989), and the remaining 2% are in filters J , G , K , r , R , y , or I . We transformed the B , V , R , I , J , K or r magnitudes into G ones using relations provided in Tables 5.8 and 5.9 of the *Gaia* DR3 documentation⁷. For ‘ P ’ and y bands we used the same relations as for transforming B and J bands, respectively, which are the closest in terms of wavelength coverage. Figure 6 presents the results of this transformation: the significant magnitude differences clearly disappear at large colour index, and the mean G difference after transformation is 0.02 ± 0.12 mag.

⁷ Section 5.5.1 Photometric relationships with other photometric systems of *Gaia* DR3 documentation.

3.2.3 Sanity checks

The process is described in details in Appendix C. In the following subsections, we present the interesting outcomes of this process.

3.2.3.1 S_{B9} orbits in higher-order systems. From the manual checking of systems potentially not resolved by *Gaia*, because having multiple S_{B9} system numbers for a given *Gaia* source, we identified:

- 76 triple systems (152 system numbers, Table E1);
- 34 quadruple systems: 32 true quadruples (65 system numbers) and possibly two ‘optical’ ones (four system numbers), all reported in Table F1;
- six multiple systems including the Trapezium in the Orion Nebula (14 system numbers, Table G1).

Regularly, such hierarchies could be part of higher-order systems, e.g. by having visible common proper-motion companions that can themselves be SB. We did not extensively search for them but they can easily be checked with the Multiple Star Catalogue (MSC, Tokovinin 2018). We identified six stellar systems having a multiplicity larger than four and with at least two subsystems with orbits reported in S_{B9} (see also Table G1):

- in the Orion Trapezium cluster, which is a crowded, optically thick region, we have θ^1 Ori A, a triple system, whose inner binary, S_{B9} 340, is an eclipsing SB1; and, located at ~ 9 arcsec, θ^1 Ori B, (S_{B9} 341), an eclipsing SB2 (SIMBAD, MSC only for θ^1 Ori A, S_{B9}).
- WDS J15382+3615: a sextuplet (3+3) where the primary triple, HIP 76563, has the inner pair being S_{B9} 1510, and the secondary triple, HIP 76566, has the inner pair being S_{B9} 1511; the outer orbit has an estimated period of about 15 ka (SIMBAD, MSC, S_{B9}).

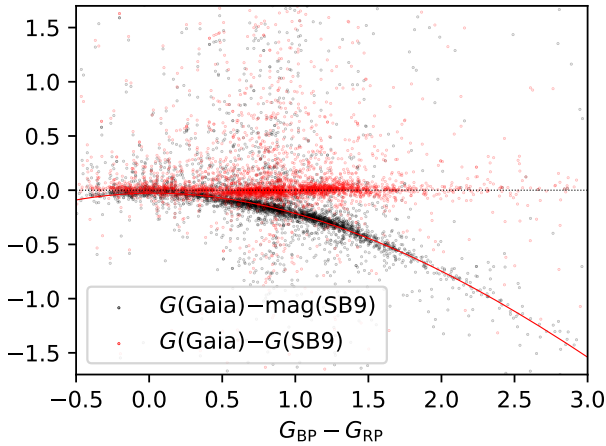


Figure 6. Magnitude differences before (black) and after (red) transformation of S_{B9} into *Gaia* magnitudes using magnitude-colour relations provided by the *Gaia* documentation.

- WDS J04357+1010: a sextuplet (4+2), where the primary is a 2+2 quadruple (88 Tau) with one of the inner orbit being S_{B9} 257, an astro-spectro-eclipsing binary, and at 70 arcsec, 88 Tau B is an SB1 (S_{B9} 1527) (SIMBAD, MSC, S_{B9}).
- WDS J18058+2127: a quintuplet (3+2), where the primary is a triple, HIP 88637, with inner pair (S_{B9} 1023, an eclipsing SB1) and outer pair (S_{B9} 1024); and the secondary is an SB2, HIP 88639 (S_{B9} 1986) (SIMBAD, MSC, S_{B9}).
- WDS J05154+3241: a quintuplet (2+3), where the primary, HIP 24504, is an SB1 (S_{B9} 305) of δ Sct type, and the secondary, HIP 24502, located at 14.25 arcsec has an SB1 in the inner orbit (S_{B9} 1484) (SIMBAD, MSC, S_{B9}).
- WDS J07346+3153: a septuplet (4+3), where the primary, Castor A, is an SB1 (S_{B9} 462) and forms a 2+2 quadruple with Castor B, another SB1 (S_{B9} 461); YY Gem, located at 70.5 arcsec, is a triple whose inner binary is an SB2 (S_{B9} 463) (SIMBAD, MSC, S_{B9}).

This investigation of high-order systems revealed that, among the 31 quadruple systems identified in S_{B9} , and reported in Table F1, 3 are complete spectroscopic quadruples, with the 3 orbits derived while the other have only 2 orbits referenced, as summarized in Table 4:

- μ Ori (Debernardi et al. 2000; Fekel et al. 2002): differential astrometry by Muterspaugh et al. (2008) allowed them to determine mutual inclinations between the orbits and to completely characterize this quadruple system.
- HD 117078 (Griffin 2011): the pair of pairs was visually resolved with speckle interferometry (Tokovinin et al. 2022).
- VW LMi (Pribulla et al. 2008), one of the tightest quadruple system known: the outer orbit period is smaller than a year. It includes a contact EB-SB2 and a detached SB2. The secular evolution of such a compact quadruple system shows an apsidal motion of the inner contact EB-SB2 (Pribulla et al. 2020).

All of these quadruple systems have a 2+2 architecture, *i.e.* two binaries orbiting each other. The two first in Table 4 are VB-SB, while the VW LMi system will be difficult to resolve astrometrically, maybe by *Gaia* at the end of the mission (Pribulla et al. 2020). However, none of them has been identified as a binary in *Gaia* DR3, with angular separations between each pair being smaller than 0.45 arcsec.

The 76 spectroscopic triple systems identified in S_{B9} are reported

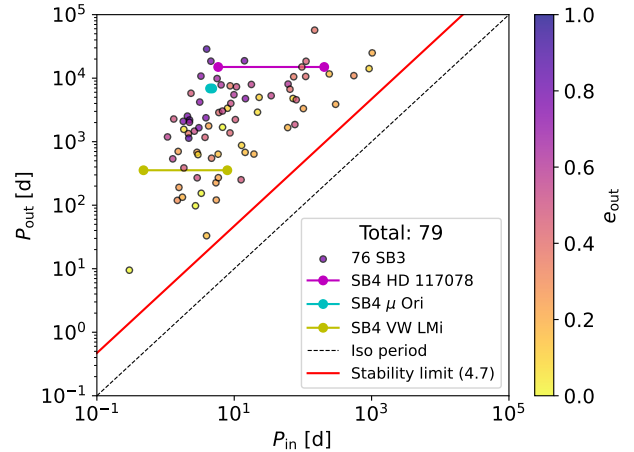


Figure 7. Outer periods vs inner period(s) of spectroscopic triple and quadruple systems in S_{B9} , colour-coded by the eccentricity of the outer orbits. The iso-period is shown by the black dashed line. The stability limit is represented by a period ratio $P_{out}/P_{in} = 4.7$.

in Table E1. Figure 7 presents their outer periods as a function of the inner ones, and colour-coded by the eccentricity of the outer orbit. The dynamical stability criterion $P_{out}/P_{in} > 4.7$ is represented by the red line and given by Tokovinin (MSC, 2018) based on Mardling & Aarseth (2001) for hierarchical triples with coplanar orbits. This figure reveals the hierarchical nature of high-order systems. Most of them are already in, or have been added (three of them) to, the MSC (Tokovinin 2018). We also added on this figure the three spectroscopic quadruples where inner and outer orbits are in the S_{B9} . Contrary to the two other spectroscopic quadruples, μ Ori has two inner orbits with very similar periods, thus having a 1:1 resonant configuration. These possible mean motion resonances (1:1, 3:2, etc.) could be important to constrain evolutionary channels to form them (Zasche et al. 2019).

Finally, we illustrate how complicated the situation can be when cross-matching and looking for high-order multiples. When multiple errors occur, it is not straightforward to disentangle them. Investigating two S_{B9} systems (1559 & 1607) with the same name in S_{B9} (BD +21 255), a potential triple or quadruple, these two systems appear to have periods of 4137 d and 1273 d, leading to a ratio of 3.2, too small to be hierarchical according to Mardling & Aarseth (2001). Component A (HIP 8876) corresponds to S_{B9} 1559 (Udry et al. 1998). Nevertheless, as many high-order systems included in S_{B9} , component B has the coordinates of component A, mixing the S_{B9} identification names. The issue here (reported in the notes of S_{B9}), is that Jorissen & Mayor (1992), while willing to observe BD +21 255 for their study on S-type stars, actually observed a K5 star located South-West at 54 arcsec (namely TYC 1212-473-1). The authors published two different orbits assigned to BD +21 255 a and b but the suffix got lost during inclusion in S_{B9} and because of this, later on SIMBAD assigned S_{B9} systems 1559 & 1607 to the same target S_{B9} BD +21° 255, while S_{B9} 1607 should point toward TYC 1212-473-1. So here we have two SB1, do they constitute a physical quadruple system? When looking at their *Gaia* DR3 parallaxes ($\varpi_A = 1.086 \pm 0.033$ and $\varpi_B = 1.531 \pm 0.024$ mas) which are significantly different, it seems that they form an optical quadruple, *i.e.* the two SB1 are not physically bound, or at least they form a very loosely bound pair of binaries. Similarly, the visual

Table 4. Details of the three complete spectroscopic quadruples in S_{B9} . They all have a 2+2 architecture and are not resolved by *Gaia* DR3.

Name	Type	S_{B9}	P [d]	e	<i>Gaia</i>	G	RUWE	Separation [arcsec]
μ Ori	A	SB1	372	4.4475858 ± 0.0000012	0.0044 ± 0.0014			
	B	SB2	373	4.7835361 ± 0.0000028	0 (Fixed)			
	AB	SB2	374	6809.9 ± 3.4	0.7426 ± 0.0020	3329650894896257024	4.674	0.27
HD 117078	A	SB1	3875	5.837891 ± 0.000008	0.0144 ± 0.0027			
	B	SB1	3876	204.256 ± 0.010	0.727 ± 0.007			
	AB	SB2	3877	15000 (Fixed)	0.374 (Fixed)	1441569596393755648	9.468	27.1
VW LMi	A	SB2	3213	$0.47755106 \pm 0.00000003$	0 (Fixed)			
	B	SB2	4003	7.93063 ± 0.00003	0.035 ± 0.003			
	AB	SB2	4004	355.02 ± 0.17	0.097 ± 0.011	733549185449902208	8.035	3.6

Notes. Separations are given between A and B systems and come from MSC (Tokovinin 2018).

Table 5. Common sample of binaries in $S_{B9} \cap Gaia$ and $S_{B9} \cap NSS$.

Catalogue	Binary	in triple	in quad	in higher-order	Total
S_{B9}	3 747	150	69	12^2	3 976
<i>Gaia</i> DR3	3 756 ⁴	76 ⁵	50	11^6	3 892
S_{B9}	800	22	4	1	827
NSS	800	11	2	1	814
Clean common sample					
S_{B9}	645	8	2	0	655
NSS	645	8	2	0	655
S_{B9}^1	3 770	152	71	14^3	4 003

Notes.

¹The numbers for S_{B9} alone are also given for reference.

²Two systems also appear in triples (S_{B9} 1023 and 1024), that is why the total is not 3978.

³Four systems also appear in triples (S_{B9} 1023 and 1024) and quadruples (S_{B9} 461 and 462), that is why the total is not 4007.

⁴Nine S_{B9} systems are resolved by *Gaia* (see Table 6).

⁵One S_{B9} triple has outer orbit resolved by *Gaia*.

⁶One *Gaia* source also appears in triples (*Gaia* DR3 4576326312902814208), that is why the total is not 3893.

pair formed by HD 179332 (S_{B9} 3839) and BD+60 1892 (S_{B9} 3840) have significantly different *Gaia* DR3 parallaxes of 5.986 ± 0.062 and 3.2511 ± 0.0307 mas, respectively. These two apparent quadruples are reported as ‘optical?’ in Table F1. While a similar conclusion is initially reached for HD 110318 (S_{B9} 735) and VV Crv (S_{B9} 734), with parallaxes of 13.895 ± 0.163 and 12.269 ± 0.053 mas, respectively, it transpires that HD 110318 and VV Crv, separated by 5 arcseconds, together form the physical binary STF 1669, which has been known for nearly 200 years (Struve 1827). The proper motion is substantial, at -0.13 arcsec a^{-1} , so the pair would rapidly move apart if it were merely an optical alignment. The discrepant parallax of VV Crv is biased and its uncertainty probably underestimated in *Gaia* DR3. There is also a third star, C (BD–12 3675, located at 59 arcsec), resulting in a total system that is quintuple.

3.2.3.2 S_{B9} system duplicates. During the manual checking process, we discovered 18 duplicates (*i.e.* two S_{B9} system numbers for the same physical binary) that should be turned into new orbit entries instead for the existing system number. Such duplicates appear most

of the time for SB in clusters. We suggest to keep the smallest S_{B9} numbers that correspond to the oldest (historical) entries in the catalogue. We suggest not to use anymore the duplicate system number to avoid any confusion in the future. As such the duplicate S_{B9} system numbers will point toward the original ones. This will allow us to keep track of their duplicate nature, while the highest system number will no longer reflect the total number of physical systems. They are listed in Table D1. These changes will be introduced in the future version of S_{B9} (see Sect. 5).

3.2.3.3 External check with SIMBAD. Finally, we ultimately compared our cross-matches (considering the previous manual corrections) with an external reference database. By comparing with the cross-match performed by the reference SIMBAD database (Wenger et al. 2000; Loup et al. 2019), we further found 15 S_{B9} systems with erroneous equatorial coordinates in S_{B9} leading to wrong best matches. This is because these SB belong to higher-order multiples and were referenced by the coordinates of the brightest component of the system, using the Washington Double Star (WDS) coordinates of the multiple, which is a convention followed by many historical databases, not only the WDS (Mason et al. 2001), but also the Sixth Catalog of Orbits of Visual Binary Stars (ORB6, Matson et al. 2006), and the Multiple Star Catalogue (MSC, Tokovinin 2018). The latter, unlike WDS, lists different coordinates for resolved components of multiple systems (not the “brightest-component” coordinates) if a given system has several entries in the MSC COMP table. One of those entries is the primary (distinguished by zero separation), the rest are “secondaries” with individual coordinates and other data, where available. We also noticed in SIMBAD a few erroneous assignments of S_{B9} systems that have since been corrected in SIMBAD. Finally, about 60 SB do not have *Gaia* DR3 identifications in SIMBAD whereas we found one for them involved in a double star. The latter is due to the fact that the cross-identification of SIMBAD with *Gaia* DR2/3 excluded objects with a neighbour within 3 arcsec of the historical position (in both SIMBAD and *Gaia*). The future version of S_{B9} and SIMBAD will be synchronized.⁸ All the S_{B9} coordinates issues reported so far will be replaced by the proper *Gaia* DR3 coordinates.

3.3 Cross-match results

Now that robust cross-matches have been secured, a statistical analysis may be performed based on the *Gaia* DR3 properties. Without the

⁸ <http://simbad.cds.unistra.fr/guide/catalogues.htm>

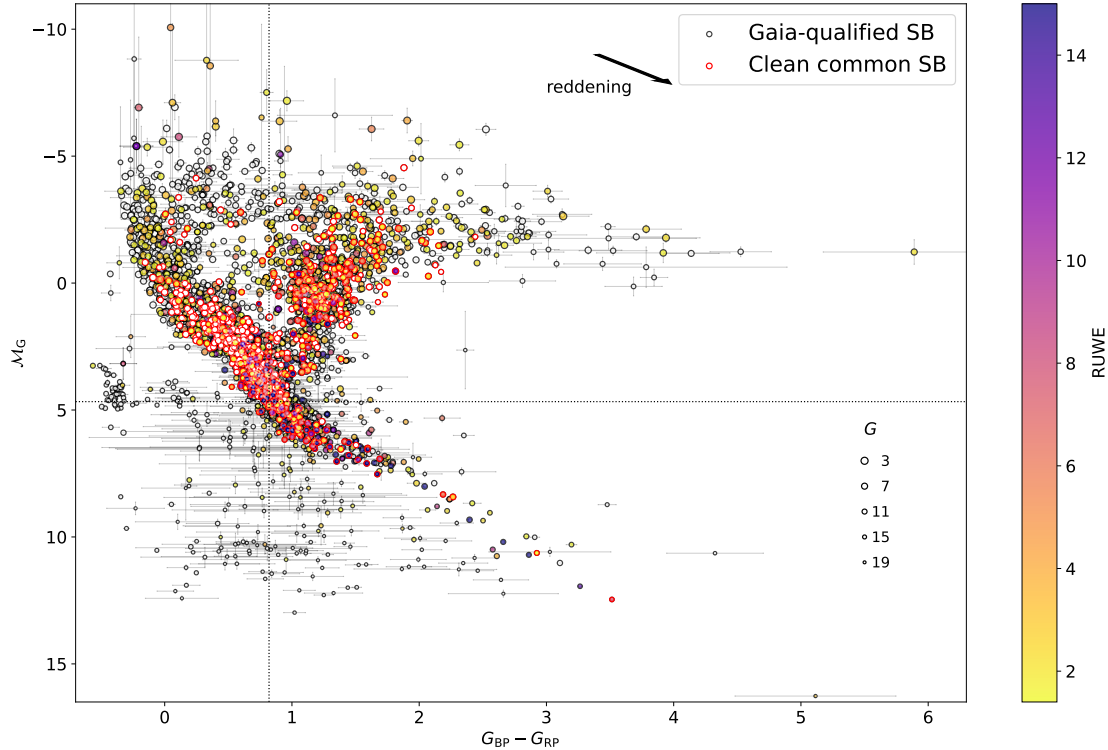


Figure 8. Colour-absolute magnitude diagram for 3781 SB (94%) of the S_{B9} catalogue with *Gaia* parallaxes, magnitudes and colors (*Gaia*-qualified SB), colour-coded by the *Gaia* DR3 RUWE value. SB with RUWE lower than 1.4 are displayed in white. The size of the symbols are related to the apparent magnitude in the G band. The position of the Sun would be at the intersection of the dotted lines. The clean common sample of 655 SB between S_{B9} and *Gaia* NSS (defined in Sect. 4.1) is shown with red circles.

18 duplicates discovered, this version of the S_{B9} catalogue (2021-03-02) contains 4003 physical spectroscopic binaries (see Table H1). Among them, 3976 have a *Gaia* DR3 counterpart (99.3%). Among them 177 S_{B9} systems do not have a parallax, 16 have a negative one and 91.7% have a parallax-over-error larger than 10. Among the 3976 S_{B9} systems with a *Gaia* DR3 counterpart:

- 916 (23%) have a radial velocity in *Gaia* DR3
- 3801 have a renormalised unit-weight error (RUWE), among which 49% have a RUWE > 1.4
- 66% have a ‘good’ astrometric fit from goodness-of-fit statistics
- 1031 (26%) are classified as binaries from the Non-Single Star catalogue (*Gaia* Collaboration 2023b):
 - Astrometric binaries (AB): 280;
 - Spectroscopic binaries (SB): 461;
 - Eclipsing binaries (EB): 62;
 - AB+SB: 212;
 - EB+SB: 16.
- 3150 have BP/RP sampled spectra
- only 250 have mean RVS spectra
- 984 (25%) show signs of variability and have epoch photometry (Mowlavi et al. 2023);
 - 452 (11%) are in the variability table of the 2 million EB candidates;
 - 3731 (94%) have atmospheric parameters from the Multiple Star Classifier based on BP/RP photometry excess; assuming unresolved co-eval binary systems (Creevey et al. 2023).

We display the colour-absolute magnitude diagram (CaMD) of

the S_{B9} catalogue in Fig. 8. 3781 SB in the catalogue (94%) have *Gaia* parallaxes, magnitudes and colours. Uncertainties on absolute magnitude were obtained by propagating errors on parallaxes and G magnitudes, the latter being derived following Eq. (12) of Merle et al. (2020). They are non-negligible for systems outside the main sequence and the red-giant branch. Systems are colour-coded by their RUWE between 1.4 and 15, with 96% of the systems having RUWE < 15. The S_{B9} system with the highest RUWE (43.3) is HD 28634 (K2V) in the Hyades cluster, which appears to be an AB (McArthur et al. 2011) and an SB1 (Griffin et al. 1985). With a period of 844.6 d, it is also characterized as an AB+SB1 in *Gaia* DR3.

For reference, the Sun would be located at the intersection of the dotted lines in the CaMD at $G_{BP} - G_{RP} = 0.82$ and $M_G = 4.67$ (Casagrande & VandenBerg 2018). The direction of the reddening, shown by the black arrow on the CaMD, is obtained from Andrae et al. (2018). The loci of the S_{B9} binaries in the CaMD have not been corrected for the reddening in Fig. 8. Main-sequence M-type binaries are under-represented in the S_{B9} . It is beyond the scope of this paper to investigate the CaMD diagram of the S_{B9} catalogue in greater detail, but various avenues for exploration could be pursued.

In the $S_{B9} \cap Gaia$ common sample, the number of unique *Gaia* DR3 sources is 3892, meaning that many spectroscopic multiples in S_{B9} are unresolved by *Gaia* DR3. In contrast, a few S_{B9} systems are resolved and are presented in Table 6.

3.3.1 S_{B9} systems resolved by *Gaia*

To determine whether some S_{B9} systems are resolved by *Gaia*, we proceed similarly to Halbwachs (1981) who estimated the angular

Table 6. Ten S_{B9} systems resolved by *Gaia* with tentative computed inclinations.

S_{B9}	SIMBAD Name	<i>Gaia</i> A	G_A	<i>Gaia</i> B	G_B	$\rho_{S_{B9}}^{\min}$ [arcsec]	ρ_{Gaia} [arcsec]	P [d]	i [°]
915 ¹	ζ Her A and B	1312665361415345920	2.716	1312665361414730624	2.763	0.38	0.26	12596.1	43
879	ξ Sco A and B	4343066192373820800	4.851	4343066192373234048	4.872	0.13	0.96	16326.3	8
1022	70 Oph A and B	4468557611984384512	3.987	4468557611977674496	5.539	3.95	6.41	32188.8	38
1470 ¹	HD 3443 A and B	2347260998051944448	5.954	2347272641708189440	6.216	0.27	0.72	9165.64	22
1472	BD+42 501 A and B	339384295642198272	9.191	339384299937913856	9.335	0.47	0.70	116675 \pm 7670	42
1478	HD 191854 A and B	2081078269591424896	7.756	2081078269585872000	8.260	0.44	0.64	31125 \pm 44	43
1815 ²	NGC 2682 131 A and B	604921546365012480	11.621	604921542069455104	11.861	0.0002	0.42	1188.5 \pm 6.7	0
2460 ³	BD+40 883 A and B	1873073175244118784	9.397	1873073175249217408	-	0.70	0.88	10777 \pm 241	53
2559 ⁴	HD 176051 A and B	2043885295914531072	5.174	2043885295914530944	7.503	0.47	1.28	22423.0	22
3657 ¹	HD 155876 A and B	1364668825433448704	8.860	1364668825433435776	9.183	0.08	1.13	4693.5 \pm 18.3	4

¹No *Gaia* parallax available, HIPPARCOS used instead (van Leeuwen 2007).

²No *Gaia* parallax available, *Gaia* cluster parallax used instead (Gaia Collaboration 2018). Primary (component A) is itself a SB and EB with system number S_{B9} 1834.

³Primary (component A) is itself a SB with system number S_{B9} 1280.

⁴B component is the host of an S-type exoplanet with 1.5 ± 0.3 Jupiter mass (Mutterspaugh et al. 2010).

Table 7. Fourteen triple-system candidates (S_{B9} inner binary with an outer *Gaia* companion). More candidates could exist in S_{B9} .

S_{B9}	SIMBAD Name	<i>Gaia</i> 1, <i>Gaia</i> 2	G_1, G_2	ϖ_1, ϖ_2 [mas]	$\rho_{S_{B9}}^{\min}$ [arcsec]	ρ_{Gaia} [arcsec]	P [d]
619	HD 91948	1047782393124538624, 1047782393123982464	6.674, 10.903	13.887 \pm 0.027, 13.835 \pm 0.015	0.0002	4.1	2.77
1414	BD+62 2155 A	2207250454387300224, 2207250458683385472	9.847, 11.100	1.197 \pm 0.014, 1.210 \pm 0.065	7×10^{-7}	1.72	1.0392
1786	HD 93161 A	5350362982543827456, 5350362982543828352	8.483, 8.471	0.340 \pm 0.028, 0.386 \pm 0.028	8×10^{-6}	2.01	5.63 \pm 0.13
1934	MM Eri B	3185860165825182592, 3185860161531606528	10.918, 10.514	6.327 \pm 0.0372, 6.256 \pm 0.0278	0.0008	1.07	13.5601 \pm 0.0012
2097	RX J0451.6+0619 A	3288074511955863424, 3288074511954439424	12.616, 14.944	3.863 \pm 0.025, 3.969 \pm 0.062	0.00003	1.16	0.6976
2112 ¹	HD 75638 A	604997202213330560, 604997206508854656	8.157, 10.116	5.623 \pm 0.052, 5.406 \pm 0.133	0.00009	2.15	5.8167 \pm 0.0009
2288	HD 96345 A	3968543807205045248, 3968543802915918464	8.989, 10.325	24.627 \pm 0.104, 24.406 \pm 0.045	0.0450	2.15	6089 \pm 1391
2339	HD 111306	1567523601159749376, 3692343531370523648	6.736, 11.807	15.536 \pm 0.046, 16.031 \pm 0.218	0.0031	1.33	61.504 \pm 0.004
2376	GD 319 A	1570548009752602240, 1570548014049174272	12.665, 13.193	4.011 \pm 0.040, 3.979 \pm 0.011	7×10^{-6}	2.62	0.6027
3068	35 Com A	3942757338955937408, 3942757334664656512	4.772, 7.074	12.065 \pm 0.288, -	0.01363	1.15	2908.25 \pm 4.27
3267 ²	UCAC4 651-076363	2076389196098727552, 2076389196100846720	14.956, 17.397	0.227 \pm 0.083, 0.314 \pm 0.095	0.00002	0.96	81.68 \pm 0.12
3509	53 Aqr	2595463992699783424, 2595463996992115840	6.098, 6.213	49.50 \pm 1.23 ³	0.00467	2.22	257.31 \pm 0.22
3813	LP 395-8 A	1829571684890816384, 1829571684890816512	11.023, 12.875	33.898 \pm 0.026, 33.896 \pm 0.053	0.00036	1.67	1.1293
3825 ⁴	HD 159027	4595342877592176512, 4595342881890087552	7.633, 13.508	2.526 \pm 0.069, -	0.00226	1.29	1359.5 \pm 1.0

Notes. Indexes 1 and 2 refer to the S_{B9} system and the suspected outer companion, respectively.

¹ Reported as a *Gaia* astrometric binary in NSS.

² Possibly an optical triple because significant different proper motions in declination at ~ 5 kpc.

³ No *Gaia* parallax available, HIPPARCOS used instead (van Leeuwen 2007).

⁴ The brightest component is detected as an astrometric binary in *Gaia* DR3 NSS; there is also a good wide companion candidate at 28 arcsec, *Gaia* DR3 4595342877593285632.

separation for 431 SBs from Batten et al. (SB7 catalogue 1978). First, we compute the absolute projected semi-major axes $a_A \sin i$ and, when it is an SB2, $a_B \sin i$. Second, we compute the relative semi-major axis $a \sin i = (a_A + a_B) \sin i$ for SB2, and $a \sin i \sim a_A \sin i$ for SB1. We further assume that, being observed as SB, $\sin i \sim 1$, which provides a lower limit for the semi-major axis a . With this estimation, and using *Gaia* parallaxes, we can guess what would be the separation in arcsec between *Gaia* sources if they were resolved. To maximize the chance of finding a resolved companion, we set the cone search radius for each system to be three times the estimated semi-major axis. We reliably find 10 systems in S_{B9} resolved by *Gaia* (see Table 6), whose S_{B9} orbital periods exceed 3 a. Among them, three resolved systems were identified when synchronising SIMBAD and S_{B9} catalogues (S_{B9} 879, 1815 and 3657). The system S_{B9} 1815 (NGC 2682 131, in the old open cluster M67) is a spectroscopic triple where the S_{B9} 1815 orbit is the outer one (representing AB pair) and S_{B9} 1834 orbit is the inner one (component A). Component A (*Gaia* DR3 04921546365012480) is itself an eclipsing binary while component B (*Gaia* DR3 04921542069455104) is a blue straggler (Van Den Berg et al. 2001). The primary of the eclipsing binary is itself a blue straggler (Sandquist et al. 2003). Components A and B are separated by 0.42 arcsec. It is the only S_{B9} spectroscopic triple partially resolved by *Gaia*. Finally, we tentatively estimate the inclination for

these resolved binaries using $i = \arcsin(\rho_{S_{B9}}^{\min} / \rho_{Gaia})$ where $\rho_{S_{B9}}^{\min}$ is the minimum estimated separation from S_{B9} orbit and ρ_{Gaia} is the separation between two *Gaia* sources. When parallaxes are not available from *Gaia*, we used the HIPPARCOS ones (van Leeuwen 2007).

3.3.2 Triple candidates with *Gaia*

In the course of identifying resolved S_{B9} systems by *Gaia*, we uncovered a certain number of triple-system candidates. We did not search extensively for them as it is not the primary goal of this paper, but report the S_{B9} systems where the minimum estimated separation $\rho_{S_{B9}}^{\min}$ are orders of magnitude smaller than the separation between two close *Gaia* sources ρ_{Gaia} . They are presented in Table 7. The S_{B9} periods of the inner pairs are reported confirming that such systems are not resolved by *Gaia*. A difference between $\rho_{S_{B9}}^{\min}$ and ρ_{Gaia} on one hand, and short periods of S_{B9} systems on the other hand, make these S_{B9} systems with close *Gaia* sources good triple system candidates. None but one (S_{B9} 2112) is detected as an astrometric binary itself in NSS with a period of 743.6 ± 10.8 d. In the S_{B9} notes, it is mentioned that this system is a triple-lined system, but only the SB1 orbit of 5.8167 ± 0.0009 d for the short-period pair is given in S_{B9} . This make the S_{B9} 2112 a probable quadruple system with the *Gaia* companion at 2.15 arcsec. We excluded one triple candidate from

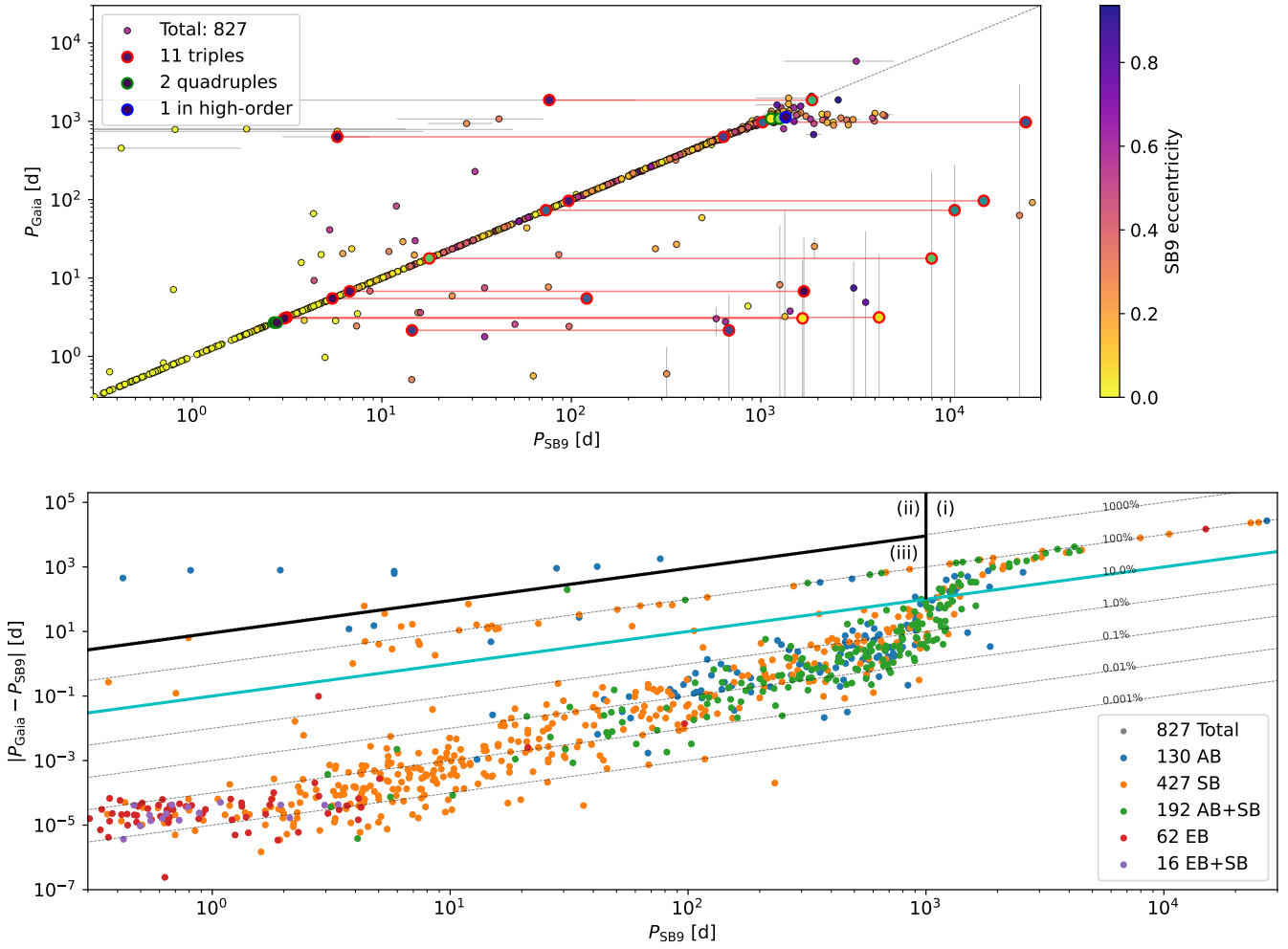


Figure 9. Comparison of orbital periods for the S_{B9} systems in common with *Gaia* NSS. Top: Log-scale comparison colour-coded with eccentricities. Bottom: absolute period differences on log-log scale. Relative difference from 0.001% to 1000% are represented with dotted grey lines. The legend shows the *Gaia* NSS binary type. The three outliers regions (i), (ii) and (iii) above the cyan line (relative period error larger than 10%) are discussed in the text.

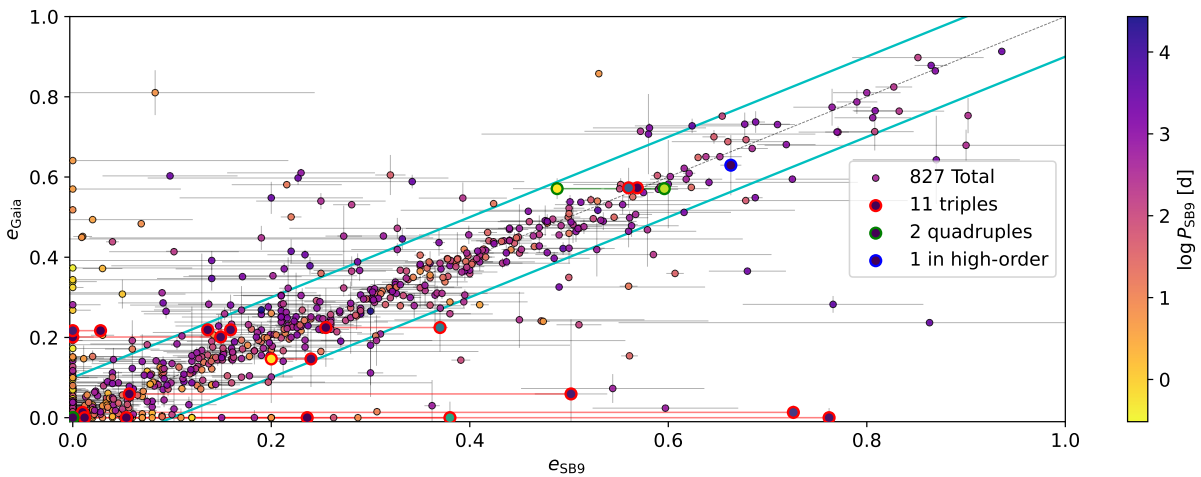


Figure 10. Comparison of eccentricities for the S_{B9} systems in common with *Gaia* NSS, colour-coded with the decimal logarithm of the period.

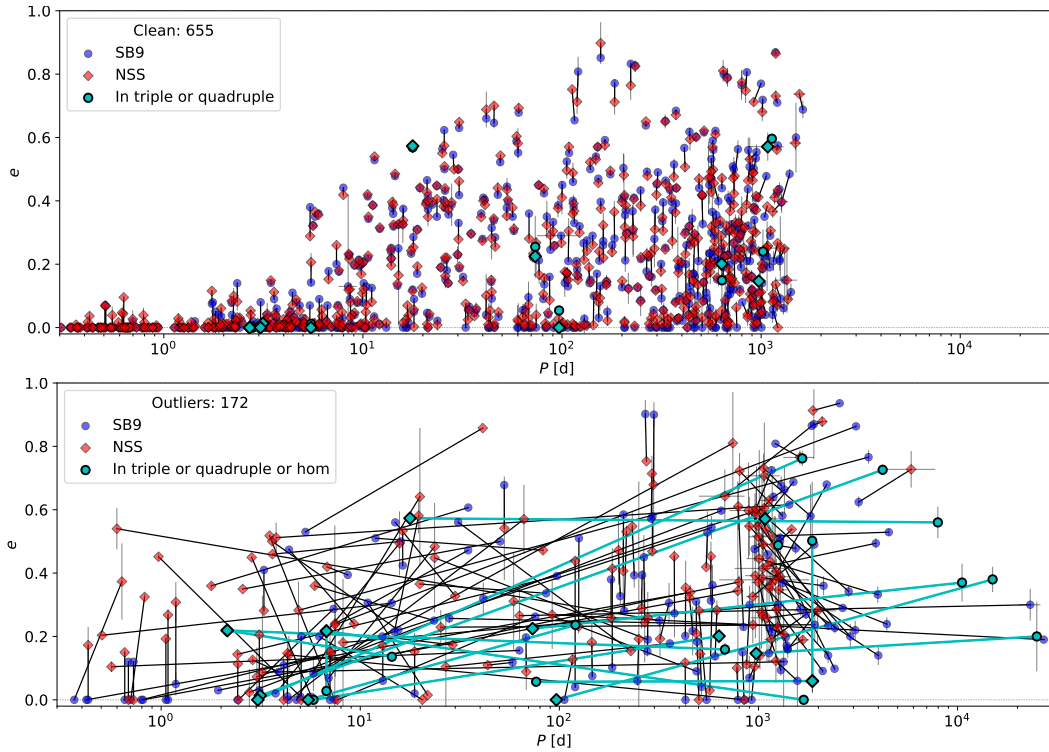


Figure 11. Eccentricity vs decimal logarithm of the period for the common S_{B9} -NSS sample of 827 binaries, 655 in the clean sample (middle), and 172 in the outliers (bottom). Orbital parameters from S_{B9} are in blue and from *Gaia* NSS in red. We connected matched binaries with black lines. Binaries in triple, quadruple or higher-order multiples (hom) are shown in cyan.

Table 7 because it is known as a quadruple (Lu et al. 2001) made of an SB1 (HD 119931 A) and an SB2 contact system (S_{B9} 2029, HD 119931 B). In Table 7, S_{B9} 3068, 3509 and 3825 are less reliable candidates because only one parallax is available, making the companion a possible ‘optical’ triple.

3.3.3 Higher-order SB (not) resolved by *Gaia*

The presence of a unique *Gaia* source for two or more S_{B9} systems means that the multiple system is not resolved by *Gaia*. E.g. S_{B9} 1524 (SB2) and 1525 (SB1) form a spectroscopic quadruple system with two visible components (Torres 2006), previously detected as a triple (Tokovinin & Gorynya 2001), this quadruple being component B of system χ Tau, the primary being a B9V star. High-order systems with S_{B9} orbits are shown in Tables E1 and F1. Among the 76 spectroscopic triples (Table E1), we found only one to be partially resolved by *Gaia*, i.e. the outer companion is resolved, not the inner pair. One spectroscopic triple (S_{B9} 157 & 158, Algol) is too bright to be observed by *Gaia*. Among the 34 spectroscopic quadruples (Table F1), half (17 quadruples) are resolved by *Gaia*, i.e. the two pairs are resolved, not the individual components. Two of them have inner binaries identified as binaries in *Gaia* DR3 NSS, i.e. TYC 1212-473-1 (S_{B9} 1607) as an NSS SB and HD 179332 (S_{B9} 3839) as an NSS AB (see Table F1). Among S_{B9} systems belonging to higher-order multiples (Table G1), we found about 14 S_{B9} systems belonging to six higher-order multiples. In the multiple system WDS 7346+3153, Castor A and Castor B are too bright for *Gaia* (see Table 2).

4 COMPARISON WITH *Gaia* DR3 NSS

We compared the S_{B9} catalogue with the *Gaia* Non-Single Star (NSS) catalogue (Gaia Collaboration 2023b), which contains the largest homogeneous sample of SB ($\sim 277\,000$) but also astrometric binaries (AB, $\sim 508\,000$) and eclipsing binaries⁹ (EB, 87 000). There are overlaps between AB, SB and EB: $\sim 58\,200$ binaries are AB+SB, 424 are SB+EB, 262 AB+EB and 17 are AB+SB+EB. We focus the cross-match on the table `nss_two_body_orbit` which provides the complete set of orbital parameters, while tables `nss_acceleration_astro` and `nss_non_linear_spectro` provide tentative and partial orbital solutions.

In S_{B9} , we select the best orbit to compare with, i.e. the ones with the highest grade (from 0 to 5¹⁰, the higher corresponding to the best one) or the most recent reference. Half of the S_{B9} orbits have no grade. In NSS, a *Gaia* source could have several orbital solutions as well, distinguished by their `nss_solution_type`. We selected as the best NSS orbit the one with the largest significance on the orbital period, i.e. the largest period-over-error value.

The intersection between S_{B9} and *Gaia* NSS produces a common sample of 827 binaries (see Table H1) which only represents $\sim 1/5$ of binaries in S_{B9} . Among them 14 are not resolved by *Gaia*: 11 triples, two quadruples and one higher-order system. For triple and quadruple systems, their S_{B9} and *Gaia* identifiers can be found in Tables E1 and F1. In this common sample, 62 have combined NSS

⁹ We do not mention the approximately 2 184 000 EB from another table, `vari_eclipsing_binary`, which provides detections and partial orbital characterisations.

¹⁰ An exception exist for α Cen (system 815), orbit number 3, with a grade of 5.1.

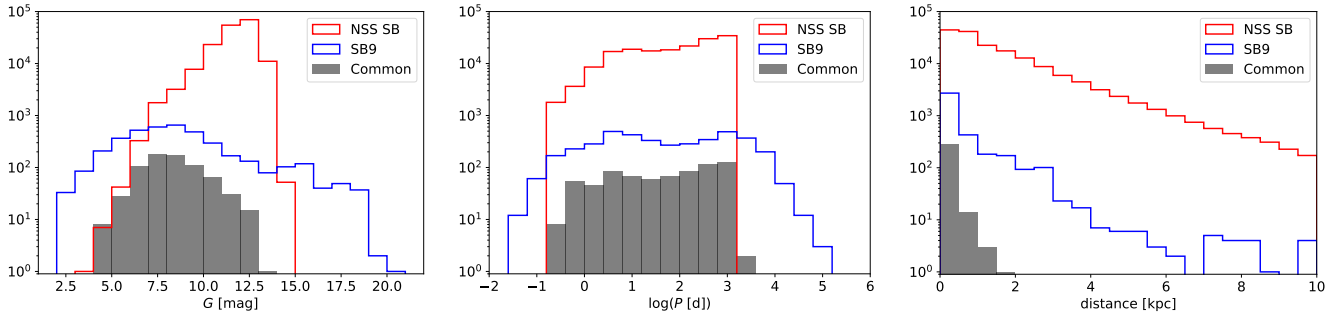


Figure 12. Magnitudes (left), period (middle) and distance (right) histograms of *Gaia* NSS SB with full orbital solutions (172k), S_{B9} (4k) and the clean common SB sample (0.66k).

orbital solutions: AB+SB for most of them and a few EB+SB. We compare S_{B9} periods with *Gaia* NSS ones in two different ways as displayed in Fig. 9. For this common sample, the tightest binary is GZ And (S_{B9} 1961) with an orbital period of 0.3 d which is also an EB. The widest pair is 26 Dra (S_{B9} 2557) with a period of 27087 d, while it is estimated to be 92.04 ± 0.29 d in NSS. The binary with the largest *Gaia* NSS period is BD+15 2570 with 5845.7 ± 1868.9 d (S_{B9} 2301 with 3186 ± 29 d). We also compare the S_{B9} and *Gaia* NSS orbital eccentricities as shown in Fig. 10, colour-coded by period. In general, the uncertainties are larger in S_{B9} . The scatter is weaker at high eccentricities. We noticed two populations on the horizontal and vertical axes corresponding to circular binaries in one catalogue that have non-null eccentricities in the other catalogue. More S_{B9} circular systems have non-null *Gaia* NSS eccentricities than vice versa.

4.1 Identifying SB outliers

Half of this common NSS – S_{B9} sample has a relative precision on the orbital period better than 0.1%. Among them, there are 16 systems both measured as eclipsing and spectroscopic binaries (EB+SB) with excellent solutions where the relative period difference is lower than 0.01%. 115 systems (14%) have relative period differences larger than 10% and are considered as outliers (systems above the cyan line in the bottom panel of Fig. 9). We can distinguish three categories among these outliers: (i) the ones due to the threshold effect (aliasing effect), (ii) outliers above the 1000% relative difference, and (iii) outliers around the 100% relative difference, *i.e.* between 10 and 1000%. The category (i) is due to a threshold effect around 1000 d, *i.e.* *Gaia* NSS binaries have periods saturating around 1000 d. This corresponds to the time span of *Gaia* DR3 based on 34 months of data collection (from 25 July 2014 to 28 May 2017). We identified 61 systems in this category. In category (ii) with relative difference larger than 10 (1000%), nine systems are detected as astrometric binaries in *Gaia* but one identified as SB1. They are all candidates triple systems with the inner binary measured as SB in S_{B9} and outer system identified by astrometry with *Gaia* (see Table 8). Two of them are spectroscopic triples in S_{B9} , namely S_{B9} 1624 & 1625 and S_{B9} 3727, 3728. The ratio of outer over inner periods ranges from 15 to 1000. The smallest ratio is the SB1 with SIMBAD identifier NGC 2682 176 in the open cluster M67. The category of outliers (iii) with relative period difference between 10 and 1000% (and S_{B9} periods lower than 1000 d) represents 45 systems mainly consisting of *Gaia* SB and AB+SB. The period ratio (*Gaia* over S_{B9}) ranges from 0.002 to 9. An illustrative example is given for S_{B9} 231 with a period ratio of 0.1 on right panel of Fig. 14 as discussed in Sect. 4.2.

When looking at the eccentricities, we consider as outliers systems that have an absolute eccentricity difference larger than 10%, *i.e.* outside the area defined by the cyan lines in Fig. 10. They represent 129 systems (16%). The intersection and combination of these two criteria (i) on relative period differences of 10%, and (ii) on absolute eccentricity differences larger than 10% provide samples of 72 and 172 systems, respectively. We will use the combination of these two criteria to determine the final set of 172 outliers representing about 21% of the common sample. Figure 11 shows how this affects the eccentricity-decimal logarithm period diagram of this common sample (827 binaries), what results as the clean sample (top panel, 655 golden binaries), and the outliers themselves (bottom panel, 172 outliers). We also noticed that all systems with periods larger than 1500 d are excluded. When checking for higher-order multiples, we identified one triple unresolved by *Gaia* (476270508301993344) where the two S_{B9} systems (216 & 2052) have very similar periods of 2.6982 and 2.7966 d. *Gaia* (476270508301993344) is identified as an EB with a period of 2.6984 d. This is why we set S_{B9} 2052 as an outlier. This clean common sample can serve as a validation sample for future surveys. It will also extend toward longer orbital periods with future *Gaia* releases.

Seven SB1 from the clean sample of 655 binaries turn out to be SB2 in NSS. Table 9 reports the semi-amplitudes, periods and eccentricities in each catalogue. For these systems in S_{B9} , no uncertainties are reported for semi-amplitude, period and eccentricity by the authors provided in the reference column, because studies are quite old. We noticed that the semi-amplitudes are significantly different between NSS and S_{B9} . Among these seven SB1, four are variable: S_{B9} 270 (RZ Eri) and S_{B9} 900 (*t* TrA) of spectral type F; and S_{B9} 1118 (BH Dra) and S_{B9} 1382 (GX Peg) of spectral type A. Five false positives also popped up among the outliers, because they are all belonging to S_{B9} spectroscopic triples unresolved by *Gaia*, matching the outer S_{B9} pair with the NSS inner pair. An interesting example is SS Lac, known as a variable since 1915, and member of the open cluster NGC 7209. It is indeed an EB with a period of 14.4 d but on an eccentric orbit ($e = 0.136$). After 1950, the eclipses fully disappeared, puzzling astronomers about the causes. Intensive investigations by Torres & Stefanik (2000) revealed that the inclination changed by 6° over 40 years, due to the gravitational effect of a distant companion (Kozai-Lidov effect) on an outer orbit of 678.8 ± 4.1 d. This spectroscopic triple system has both inner and outer orbits in S_{B9} (S_{B9} 2456 & 2458). It is not only unresolved by *Gaia*, but the inner SB2 orbital solution provides a period of 2.1 d with an eccentricity of 0.22 which is at odds with Torres & Stefanik (2000) determination.

A similar study was conducted on a sample of about 100 triple stars

Table 8. Nine unresolved triple candidates with S_{B^9} inner spectroscopic orbit and *Gaia* NSS outer astrometric orbit.

SIMBAD	S_{B^9}	$P_{S_{B^9}}$ [d]	$e_{S_{B^9}}$	<i>Gaia</i> DR3	G	P_{Gaia} [d]	e_{Gaia}
63 Gem	454	1.9327	0.03	865209037088705024	5.099	798.4 ± 11.4	0.372 ± 0.020
HD 83270	1624 ¹	5.8214	0	1070770191963666816	7.466	633.6 ± 2.8	0.201 ± 0.021
NGC 2682 176	1821	4.3556 ± 0.0002	0	604916422468464768 ²	12.476	66.38 ± 0.28	0.570 ± 0.109
ϕ Phe	1916	41.489 ± 0.019	0.32 ± 0.05	4957620109130881664	5.096	1070.4 ± 29.5	0.605 ± 0.015
V899 Her	2024	0.4212	0	1325067886936436224	7.773	454.3 ± 1.4	0.339 ± 0.024
HD 75638A	2112	5.8167 ± 0.0009	0.0830 ± 0.056	604997202213330560	8.157	743.5 ± 10.8	0.810 ± 0.161
HD 150710	2677	28.01 ± 0.012	0.257 ± 0.014	1312345747129055744	6.938	938.5 ± 10.5	0.237 ± 0.005
V335 Peg	2977	0.8107	0	2717981134566374272	7.149	787.7 ± 48.4	0.344 ± 0.346
BD+60 585	3727 ¹	76.433 ± 0.014	0.057 ± 0.016	464891250151058816	8.779	1865.4 ± 143.2	0.059 ± 0.0365

Notes. They all appear as outliers of the common sample and are consequently out of the clean common sample.

¹ Member of a S_{B^9} spectroscopic triple (1624, 1625) or (3727, 3728).

² Identified as SB1 in NSS.

Table 9. Seven SB1 in the clean sample that are SB2 in *Gaia* NSS.

SIMBAD	K_1 [km/s]	P [d]	e	Ref.	<i>Gaia</i> DR3	K_1 [km/s]	K_2 [km/s]	P [d]	e
149	58.1	6.6383	0.07	(1)	461559592481317760	67.01 ± 0.21	79.57 ± 0.3	6.637771 ± 0.0000065	0.0096 ± 0.0022
197	32.4	16.725	0	(2)	66507469798631808	39.86 ± 0.38	70.23 ± 0.68	16.7402 ± 0.0012	0.0698 ± 0.0088
270	25.8	39.2807	0.36	(3)	3184295870015339264	54.09 ± 0.26	52.28 ± 0.10	39.2839 ± 0.0016	0.3485 ± 0.0021
900	38.7	39.888	0.28	(4)	5828317422956035072	38.26 ± 0.15	46.95 ± 0.20	39.8429 ± 0.0011	0.2736 ± 0.0033
906	20.3	31.846	0.16	(5)	6017724140678769024	34.33 ± 0.14	30.32 ± 0.15	31.8004 ± 0.0011	0.1464 ± 0.0025
1118	86.5	1.8172	0.05	(6)	2153474650639369600 ¹	157.73 ± 1.95	112.94 ± 7.16	1.817470 ± 0.000035	0
1382	84.9	2.341	0.02	(7)	1882432630526896000	124.63 ± 0.48	85.71 ± 0.63	2.340895 ± 0.000013	0.0318 ± 0.0040

Notes. All these values appear as outliers of the common sample and are therefore outside the clean common sample.

¹ Circular SB2 in NSS.

(1) Wellmann & Wellmann (1960) – (2) Pearce & Hill (1975) – (3) Cesco & Sahade (1945) – (4) Spencer Jones (1928) – (5) Bopp et al. (1970) – (6) Yavuz (1968) – (7) Bolton & Geffken (1976)

monitored through the CHIRON spectroscopic program (Tokovinin 2023). Among these, only about 30 systems have counterparts in the *Gaia* DR3 NSS catalogue. The comparison reveals notable discrepancies: nine of these systems show different radial velocity amplitudes between the CHIRON spectrograph ($R \sim 80\,000$) and *Gaia* NSS solutions, indicating an underestimation of the velocity amplitudes in *Gaia* likely due to blending or insufficient resolution of spectral lines. Furthermore, some systems that CHIRON identifies as SB2 remain unresolved as SB2 in *Gaia* data, affecting the completeness and accuracy of orbital characterization. One system exhibits a period alias in *Gaia* NSS, where the reported period is much shorter than the true period determined from ground-based observations. These findings confirm that, while *Gaia* NSS is invaluable for large-scale surveys, dedicated ground-based spectroscopic monitoring remains essential for detailed and reliable orbital solutions in cases of complex hierarchical systems such as triples, where *Gaia*'s automated pipeline struggles with blended or multiple-component spectra, and period aliasing.

4.2 Comparing orbital solutions

In Fig. 9, we showed that about 50% of the common binaries have a relative precision better than 0.1% on the orbital period. We illustrate two cases from the clean sample at moderate and null eccentricities (Fig. 13). 64 Psc (left panel) is an SB2 with a period of two weeks and a moderate eccentricity of 0.24. The orbital parameters of S_{B^9} and NSS are in excellent agreement, with more precise parameters from NSS which relies on 24 epochs, compared to 35 observations in Duquennoy & Mayor (1991), but spanning 4 months only. A second example from the clean sample, V1423 Aql (right panel of Fig. 13), is

an SB2 on a quasi-circular orbit of 5.4 d. We notice here a phase shift which could be explained by the fact that the S_{B^9} solution (Griffin & Fekel 1990) assumed a circular orbit (null eccentricity and periastron argument) while NSS provides a non-null eccentricity and periastron argument ($e = 0.0087 \pm 0.0011$ and $\omega = 33.3 \pm 5.9^\circ$).

We also show two cases from the outliers in Fig. 14. While the centre-of-mass velocities are in excellent agreement, the orbital elements are different. The first example is a symbiotic star AG Dra (left panel, an SB1). The relative difference in orbital period is lower than 10% but while Fekel et al. (2000) assumes a circular orbit, NSS derived an eccentric orbit with $e = 0.282 \pm 0.028$. A phase shift is also present; the time span of the observations is about 6600 d, covering about 12 cycles. The second outlier example is V1232 Tau (HIP 20056) from the Hyades open cluster, which is an SB2 with a period of 76 d and an eccentricity of 0.263, identified to have a 7.7 d period with a null eccentricity in NSS (with 20 good observations). The S_{B^9} solution covers a time span of about 2400 d, involving about 30 orbital cycles. The semi-amplitudes of the NSS solution are significantly smaller. This is a typical example where the S_{B^9} solution seems more reliable than the *Gaia* one.

Finally we compare the spectroscopic orbital parameters for a subsample (494) of the clean common sample. We selected all common binaries with `nss_solution_type` of SB1 (250), SB1 with astrometric solution (104), SB2 (110), circular SB2 (25) and spectroscopic binaries with eclipses (5). For them, we plotted the differences ($Gaia - S_{B^9}$) in semi-amplitudes K , centre of mass velocities V_0 , periods P , eccentricities e , periastron argument of the primaries ω , and in projected semi-major axis $a \sin i$ on Fig. 15. Overall, thanks to the selection in relative period and absolute eccentricity difference of 0.1, the agreement is rather good with

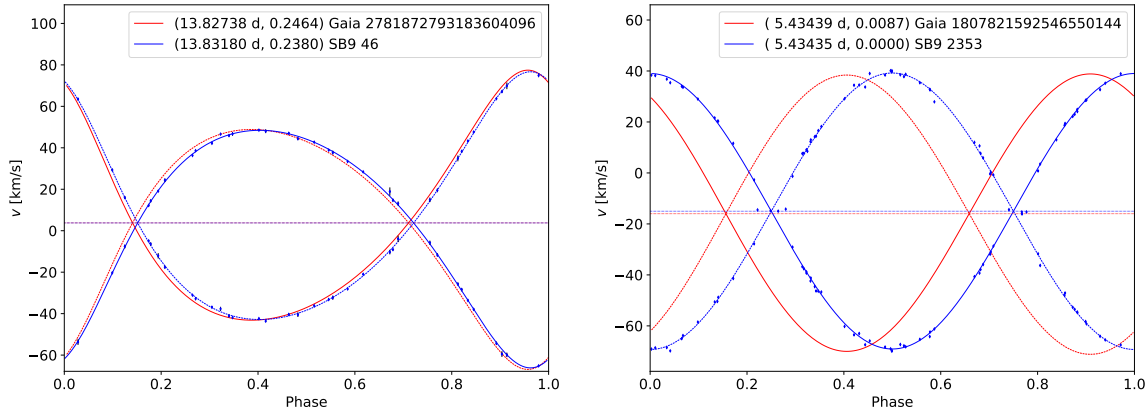


Figure 13. Comparison of RV curves for two close SB2 in the clean sample. Period and eccentricity are given in parenthesis in the legend. Only RV measurements from S_{B9} are available. Horizontal dotted lines are the center-of-mass velocities. Left: 64 Psc (HIP 3810) with an S_{B9} orbital solution from [Duquenoey & Mayor \(1991\)](#). Right: V1423 Aql (HIP 99210) with an S_{B9} orbital solution from [Griffin & Fekel \(1990\)](#).

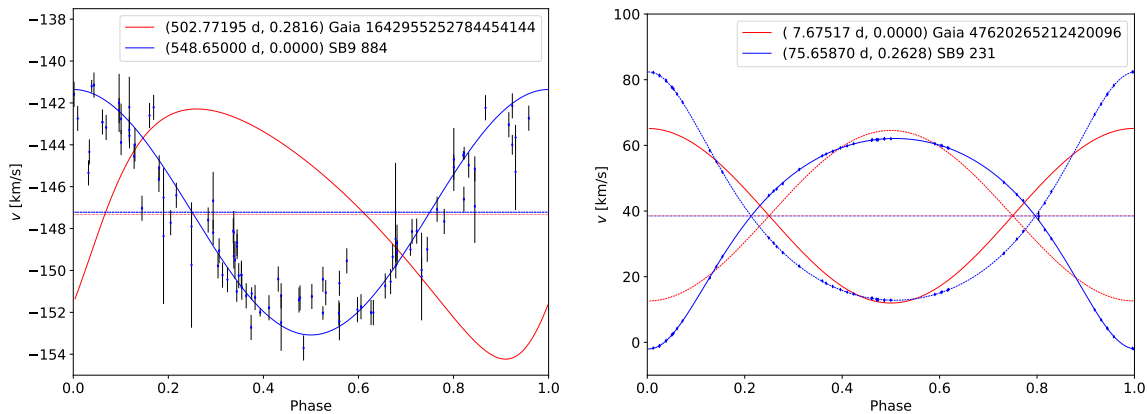


Figure 14. Comparison of RV curves for two SB identified as outliers. Left: AG Dra (HIP 78512), a symbiotic star, with an orbital solution from [Fekel et al. \(2000\)](#), 4 orbits exist in S_{B9} . Right: V1232 Tau, member of the Hyades open cluster, with an orbital solution from [Tomkin \(2003\)](#).

$\langle \Delta K_1 \rangle = 2.0 \pm 9.3 \text{ km s}^{-1}$ and $\langle \Delta K_2 \rangle = -4.7 \pm 13.8 \text{ km s}^{-1}$; $\langle \Delta V_0 \rangle = 0.1 \pm 2.6 \text{ km s}^{-1}$; $\langle \Delta P \rangle = -1.9 \pm 14.3 \text{ d}$; $\langle \Delta e \rangle = (2.4 \pm 31.0) \times 10^{-3}$; $\langle \Delta \omega \rangle = 7 \pm 69^\circ$; and $\langle \Delta(a_1 \sin i) \rangle = (0 \pm 18) \times 10^{-3} \text{ au}$ and $\langle \Delta(a_2 \sin i) \rangle = (-3 \pm 7) \times 10^{-3} \text{ au}$.

4.3 Why is the common sample so small?

The clean common sample of 655 golden binaries is composed, in NSS, of 81 AB, 351 SB, 151 SB+AB, 57 EB, and 15 SB+EB. We show in Fig. 12 the comparison between the magnitudes (left), the periods (middle), and the distances (right) of *Gaia* NSS, S_{B9} and the clean common sample of SB. The NSS SB are the ones with full spectroscopic orbital solutions (*i.e.* excluding SB with non-linear trends from the *Gaia* nss_non_linear_spectro catalogue). There are about 172k and cover a magnitude range of [3.5, 14.4], smaller than the SB from S_{B9} . Indeed, S_{B9} has 4k SB in the V magnitude range [-1.46, 26.9], but in the plotted histogram, this range is reduced to G magnitudes [2.1, 20.9] excluding the too bright and too faint stars that are not in *Gaia*, and summarized in Tables 2 and 3.

The histogram of periods in the middle panel of Fig. 12 clearly show that many S_{B9} systems have shorter or longer periods compared to SB from NSS. The common sample covers the same range of

orbital periods as the parent NSS SB distribution. There are two SB from the clean common sample with periods larger than 1400 d: BD+75 523, S_{B9} 2263 ($1620 \pm 7 \text{ d}$ for S_{B9} and $1558 \pm 110 \text{ d}$ for NSS) with an NSS AB+SB solution; and the red giant 28 Ori, S_{B9} 2844 ($1496 \pm 15 \text{ d}$ for S_{B9} and $1487 \pm 100 \text{ d}$ for NSS) with an NSS AB solution. This is why they appear with larger periods compare to the NSS SB sample in red, in the middle panel of Fig. 12.

The clean common sample represents only 23% of the S_{B9} binaries on the same period-magnitude-limited sample with G magnitudes in [4.2, 13.0] and periods in [0.3, 1558] d range. We investigated why the common fraction between S_{B9} and *Gaia* NSS is so small. There is not a unique answer and it turns out that many factors are responsible for this. (i) S_{B9} systems brighter than $G \sim 3$ represents ~ 130 systems, *i.e.* 3% of S_{B9} systems. (ii) 11% of S_{B9} binaries have $G > 13$ and hence are impossible to be observed as SB with the *Gaia* RVS. (iii) 22% of S_{B9} binaries have periods exceeding 1000 d and consequently are possibly not in NSS or appearing as outliers with relative period difference $> 10\%$. (iv) Early-type binaries (with $T_{\text{eff}} \geq 10000 \text{ K}$) are over-represented in S_{B9} and under-represented in NSS, as clearly depicted in Fig. 16. The bottom panel shows that the completeness, defined as the ratio of the common sample over S_{B9} systems per bin of effective temperature, is about 30% for FGK primaries; it

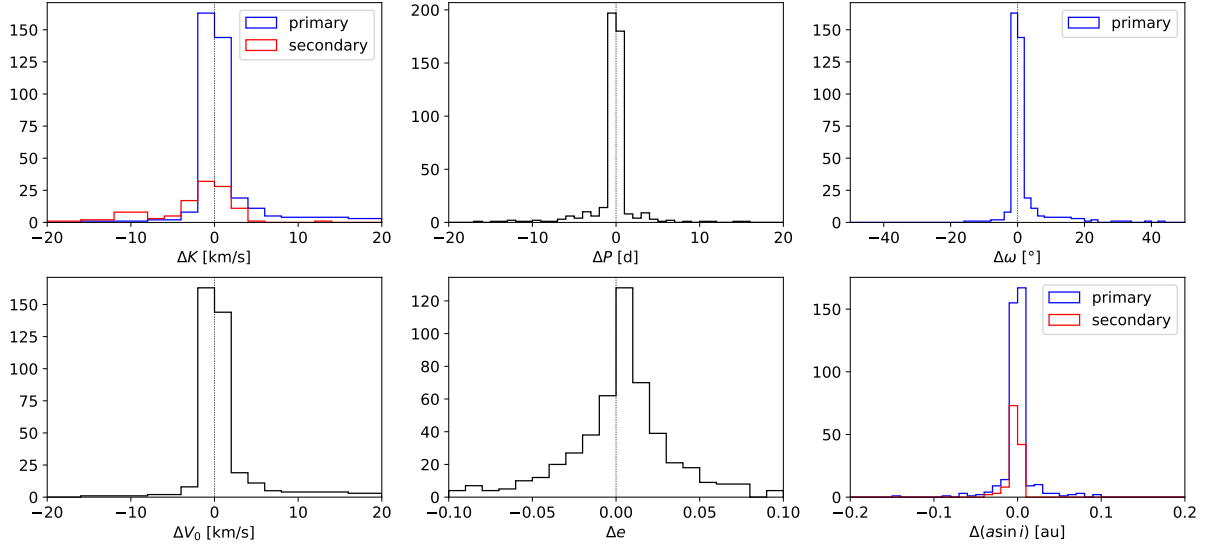


Figure 15. Histograms of the differences ($Gaia - S_{B9}$) in orbital parameters for a subsample of 494 SB of the clean common sample.

strongly decreases for M and early-type primaries. Most of them also appear as short period binaries, and S_{B9} have more SB with $K_1 \geq 150 \text{ km s}^{-1}$ as seen in Fig. 17. (v) We identified one important source of incompleteness: binaries for which an astrometric motion is present. According to Gosset et al. (2025): “Since the RVS is a slitless spectrometer, the calibration in wavelength of the spectra is requesting an epoch position of the object that is accurate enough. Therefore, for the objects that are deviating from the single star behaviour, we could expect that the wavelength calibration is not correct, and thus the measured transit RVs are somewhat biased and this creates artefacts in the time series. No correction of this effect is offered for DR3.” Subsequent strong selection cuts are performed in the analysis of SB1, with a conservative approach, rejecting binary solutions if $F_2 > 3$, if the phase coverage has a gap larger than 0.3, if $K \geq 250 \text{ km s}^{-1}$, etc. (see Gosset et al. 2025, for more details). (vi) Finally, when we cross-match S_{B9} with $Gaia$ spectroscopic orbital trends which include about 56.8k systems, we only found 56 common systems. Among the 338k $Gaia$ systems with astrometric acceleration solution, i.e. systems with non-linear proper motion, we found 206 systems in common. Comparing with these partial orbital solutions only account for 7% of S_{B9} . Contrary to Beck et al. (2024), we never reached a completeness of 40%, even in the same period-magnitude-limited sample¹¹ for which we only obtained 24% instead of 23% completeness. This is mainly due to the fact that they only identified 3413 unique S_{B9} (while we have 3976 unique S_{B9} systems corresponding to 3892 unique $Gaia$ identifiers, see Table H1, because 10 S_{B9} are resolved by $Gaia$, see Table 6).

The clean common SB sample is represented on the CaMD (Fig. 8) with magnitudes brighter than 13 and not only covers the main sequence but also the red giant branch. In addition, all the SB systems in the clean common sample are closer than 2 kpc, while 73% of NSS SB and 92% of S_{B9} systems meet this criterion. We also note

that 99.6% of S_{B9} systems and 99.2% of $Gaia$ NSS SB are located within 10 kpc.

Finally we show the distribution on the sky of $Gaia$ NSS, S_{B9} and the clean common sample of SB in a Mollweide projection in equatorial coordinates (Fig. 18). While the $Gaia$ SB show an over-density in the Galactic plane, the S_{B9} systems show an under-density in the southern hemisphere, which is also the case for the clean common sample, and is mainly due to historical observations made in the northern hemisphere.

5 EVOLUTION OF S_{B9} TOWARDS A NEW VERSION: S_{BX}

The modernization and extension of the S_{B9} catalogue has recently taken a decisive step forward. Building on the limitations identified in the legacy S_{B9} infrastructure (namely, flat file storage, inconsistent data formatting, limited search capabilities, and inflexible user interfaces), our work has led to the creation of the S_{BX} (*The eXtended Catalogue of Spectroscopic Binary Orbits*¹²), a scalable, standards-compliant platform designed to support the next decades of research on binary stars.

At the core of this transformation is the migration of the entire catalogue to a modern PostgreSQL relational database. The new schema, designed with domain best practices, enforces primary/foreign key constraints, normalization of system and orbit tables, and type safety for all physical and bibliographic parameters. Historical inconsistencies, ranging from missing values and typographical errors, were systematically resolved through custom preprocessing scripts and cross-validation against source literature and external catalogues. This new version enables more reliable and complex queries, eliminates duplicates, and establishes a solid foundation for future extensions. Details of this migration and the new implementation can be found on the S_{BX} ¹³.

¹¹ We have the same G magnitude range but they used a maximum period of 1100 d.

¹² Already available at <http://astro.ulb.ac.be/sbx>

¹³ <http://astro.ulb.ac.be/sbx/intro>

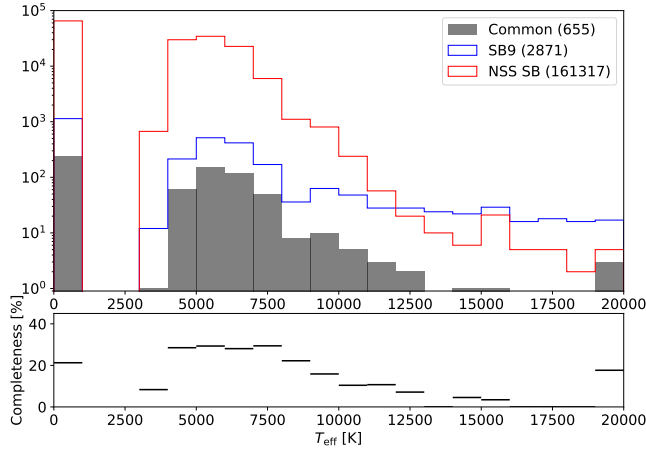


Figure 16. Top: comparison of T_{eff} (from Gaia DR3 GSPphot) distribution for NSS spectroscopic binaries (red), S_{B9} systems (blue) and the clean common sample of binaries (grey). The samples are selected on the same G magnitudes [4.2, 13.0] and period [0.3, 1558] d ranges of the clean common sample. At 0 K are shown the amount without any T_{eff} . Bottom: completeness in S_{B9} .

A key enhancement in S_{Bx} is the systematic enrichment of astrometric and photometric parameters using external resources, mainly *Gaia* DR3. High-precision positions, proper motions, parallaxes, and G magnitudes are now included for nearly all systems for which cross-identification is possible; fallbacks to HIPPARCOS and SIMBAD ensure completeness for the brightest (Table 2) and faintest binaries (Table 3). Data provenance is explicitly tracked, and new data fields document the source and reliability of each entry.

Complementing the new database, S_{Bx} features a modern, Python-based web application (using Django framework¹⁴) that vastly expands search, visualization, and data export capabilities. The new interface allows: (i) robust and resilient object lookup by name, coordinate (cone search), or alias, including fuzzy matching and integration with the CDS Sesame resolver; (ii) immediate access to all orbital solutions, notes, and bibliographic references for a given system; (iii) interactive and downloadable plots of radial velocity curves, with uncertainties and phase folding, generated dynamically on the server; (iv) direct download of measurements in CSV format; and (v) a portal (under development) for user-submitted orbit solutions with workflow for data validation and review. This architecture ensures a clear separation data, logic, and presentation, making future updates and extensions straightforward.

Recognizing the necessity for seamless integration with virtual observatory (VO) tools, S_{Bx} provides a Table Access Protocol (TAP) service compliant with International Virtual Observatory Alliance (IVOA) recommendations (Osuna et al. 2008). Powered by a dedicated TAP/ADQL middleware (using the `vo11t` library, Mantelet et al. 2023), this service enables standardized batch querying and cross-matching for external platforms, pipelines, and visualization tools (e.g., Topcat). This opens the catalogue to large-scale, federated, and automated scientific workflows, and reduces integration friction for external astronomical data centres.

While S_{Bx} represents a major leap in technical capability and scientific usability, ongoing and future efforts will focus on several fronts. (i) Complete the missing RV data for 910 S_{B9} systems (23%

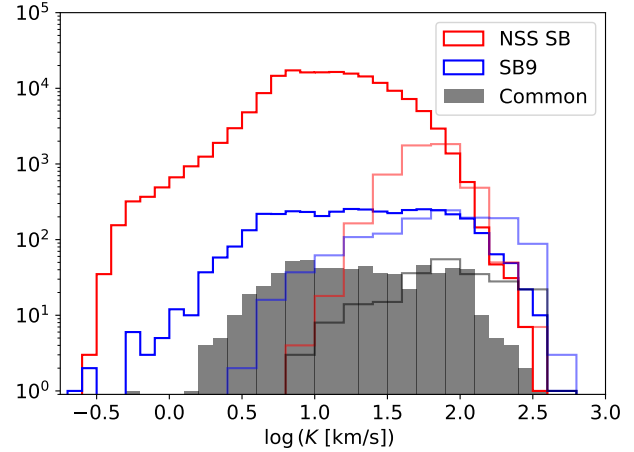


Figure 17. Semi-amplitude of the primaries for NSS spectroscopic binaries (red), S_{B9} systems (blue) and the clean common sample of binaries (grey). Semi-amplitudes of the secondaries are shown with light red, blue and grey, for the corresponding samples.

of the full catalogue). On a larger effort basis, it would also be welcome to add the list of ~ 300 references selected from 1987 to 2002 into S_{Bx} . (ii) Where possible, provide the missing uncertainties on the orbital parameters; for example, 35% of the periods and 47% of the eccentricities lack quoted uncertainties. (iii) Implement a new grading scheme for the quality of the orbits. The previous grading scheme was empirical and subjective to the contributor to the S_{B9} catalogue. The idea is to use objective criteria to assess the quality of an orbit: small uncertainties on the radial velocities, and good sampling of the orbital phase. The last one may be tricky to define for eccentric orbits. We could rely on the eccentric anomaly by imposing an anomaly gap smaller than a given value. Another option could be to define four grades: A – all orbital parameters constrained; B – some orbital parameters constrained; C – orbital parameters unconstrained; D – wrong parameters/no SB. Various options still need to be more carefully investigated before concrete implementation. (iii) Complete spectral type and luminosity class and add atmospheric parameters (effective temperature, gravity and metallicity for one (SB1) or both (SB2) components when available elsewhere (e.g. from the *Gaia* atmospheric parameters, or other large spectroscopic surveys). The future addition of interactive front-end components, advanced filtering, and visualization will improve user experience for data exploration.

The S_{Bx} website ensures that the catalogue of spectroscopic binaries has evolved from a legacy static archive to an open, dynamic, and interoperable research infrastructure, fully aligned with big data astronomy and VO best practices. This transformation puts the new S_{Bx} catalogue at the heart of future developments in stellar astrophysics, binary star population studies, and multi-catalogue synergy.

6 CONCLUSION

The S_{B9} catalogue is a comprehensive compilation of approximately 4 000 spectroscopic binary systems, consisting of about 2 800 single-lined (SB1) and 1 200 double-lined (SB2) binaries gathered from literature. This work presents the current status of the S_{B9} catalogue as of 2021-03-02, *i.e.* more than 20 years after the reference article by Pourbaix et al. (2004), including its detailed statistical properties

¹⁴ <https://djangoproject.com>

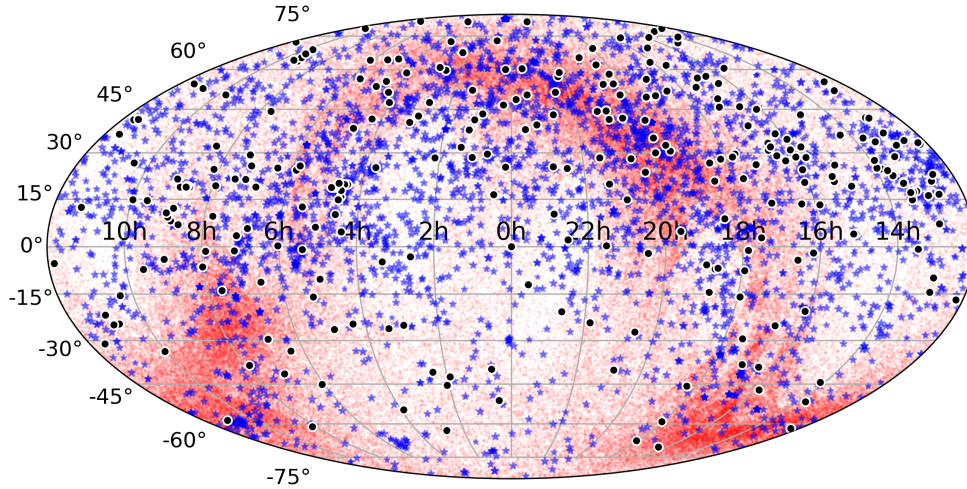


Figure 18. Mollweide projection of *Gaia* NSS (light red dots), S_{B9} (blue stars) and clean common sample (black circles) of SB in equatorial coordinates.

such as distributions of orbital periods, eccentricities, spectral types and luminosity classes of both primary and secondary stars. A major part of this study is the careful cross-match of S_{B9} with the *Gaia* DR3 catalogue, revealing 3 976 common sources and highlighting the complexities of matching binaries across catalogues with issues such as duplicates and unresolved multiples. The comparison with *Gaia* NSS shows partial overlap with insights into orbital parameters consistency and discrepancies. We identified a clean common sample of 655 systems which includes eight binaries in spectroscopic triples and two binaries in quadruple systems. We identified higher-order multiples (76 triples, 34 quadruples, and six higher order systems in which SB are present) within S_{B9} and discussed systems resolved or unresolved by *Gaia*. Importantly, this work results in the transition from S_{B9} to the modernized S_{Bx} (extended) catalogue, featuring a relational SQL database, improved web interface, and Virtual Observatory access standards, aiming to enhance accessibility, data quality, and analysis capabilities for the binary and multiple star community. The evolution of S_{B9} into S_{Bx} addresses data completeness, includes coordinates and astrometric parameters from *Gaia* DR3, as well as a new table for parents and children binaries in hierarchies, paving the way for future large-scale binary star research.

ACKNOWLEDGEMENTS

We thank the referee for constructive remarks that help to improve the readability of the manuscript. We thank E. Gosset, C. Babusiaux and O. Malkov for useful discussion and user feedback on the S_{B9} catalogue. T.M. is granted by the BELSPO Belgian federal research program FED-tWIN under the research profile Prf-2020-033_BISTRO. J.S. acknowledges support from STFC under grant number ST/Y002563/1. This research has made use of the SIMBAD database, operated at CDS, Strasbourg, France (Wenger et al. 2000). All the previous contributors to S_{B9} are warmly thanked: R. Griffin, J.M. Carquillat, M. Imbert, L. Szabados, D. Stickland, E. Glushkova, and R. Leiton. Deep gratitude to D. Pourbaix, who passed away too soon, for bringing the S_{B9} catalogue into the digital age and enriching it beyond all other contributors. This work has made use of data from the European Space Agency (ESA) mission *Gaia* (<https://www.cosmos.esa.int/gaia>), processed by the *Gaia* Data Processing and Analysis Consortium (DPAC, <https://www.cosmos.esa.int/web/gaia/dpac/consortium>). Funding for the DPAC has been provided by national institutions, in particular the institutions participating in the *Gaia* Multilateral Agreement.

DATA AVAILABILITY

Table H1 will be available online. All the data of this work can be retrieved on the S_{Bx} website and its associated TAP service at <https://astro.ulb.ac.be/sbx>.

REFERENCES

- Abt H. A., 2009, *ApJS*, **180**, 117
 Abushattal A. A., Alrawashdeh A. A., Kraishan A. F., 2022, *Communications of the Byurakan Astrophysical Observatory*, **69**, 251
 Andrae R., et al., 2018, *A&A*, **616**, A8
 Anguita-Aguero J., Mendez R. A., Clavería R. M., Costa E., 2022, *AJ*, **163**, 118
 Barker A. J., 2022, *ApJ*, **927**, L36
 Barnard E. E., 1916, *AJ*, **29**, 181
 Bataille M., Libert A. S., Correia A. C. M., 2018, *MNRAS*, **479**, 4749
 Batten A. H., 1967, *Publications of the Dominion Astrophysical Observatory Victoria*, **13**, 119
 Batten A. H., Fletcher J. M., Mann P. J., 1978, *Publications of the Dominion Astrophysical Observatory Victoria*, **15**, 121
 Batten A. H., Fletcher J. M., MacCarthy D. G., 1989, *Publications of the Dominion Astrophysical Observatory Victoria*, **17**, 1
 Beck P. G., et al., 2024, *A&A*, **682**, A7
 Belokurov V., et al., 2020, *MNRAS*, **496**, 1922
 Bolton C. T., Geffken N., 1976, *PASP*, **88**, 195
 Bopp B. W., Evans D. S., Laing J. D., Deeming T. J., 1970, *MNRAS*, **147**, 355
 Campbell W. W., 1910, *Lick Observatory Bulletin*, **181**, 17
 Campbell W. W., Curtis H. D., 1905, *Lick Observatory Bulletin*, **79**, 136
 Casagrande L., VandenBerg D. A., 2018, *MNRAS*, **479**, L102
 Cesco C. U., Sahade J., 1945, *ApJ*, **101**, 370
 Crampton D., Cowley A. P., Stauffer J., Ianna P., Hutchings J. B., 1986, *ApJ*, **306**, 599
 Creevey O. L., et al., 2023, *A&A*, **674**, A26
 Debernardi Y., Mermilliod J. C., Carquillat J. M., Ginestet N., 2000, *A&A*, **354**, 881
 Duchêne G., Kraus A., 2013, *ARA&A*, **51**, 269
 Duquennoy A., Mayor M., 1991, *A&A*, **248**, 485
 Eggleton P. P., 1983, *ApJ*, **268**, 368
 Eggleton P. P., Tokovinin A. A., 2008, *MNRAS*, **389**, 869
 El-Badry K., Rix H.-W., Heintz T. M., 2021, *MNRAS*, **506**, 2269
 El-Badry K., et al., 2023, *MNRAS*, **518**, 1057
 Fabricius C., Høg E., Makarov V. V., Mason B. D., Wycoff G. L., Urban S. E., 2002, *A&A*, **384**, 180

- Fabrycky D., Tremaine S., 2007, *ApJ*, **669**, 1298
- Feissel M., Mignard F., 1998, *A&A*, **331**, L33
- Fekel F. C., Hinkle K. H., Joyce R. R., Skrutskie M. F., 2000, *AJ*, **120**, 3255
- Fekel F. C., Scarfe C. D., Barlow D. J., Hartkopf W. I., Mason B. D., McAlister H. A., 2002, *AJ*, **123**, 1723
- Frankowski A., Jancart S., Jorissen A., 2007, *A&A*, **464**, 377
- Gaia Collaboration 2016, *A&A*, **595**, A1
- Gaia Collaboration 2018, *A&A*, **616**, A10
- Gaia Collaboration 2023a, *A&A*, **674**, A1
- Gaia Collaboration 2023b, *A&A*, **674**, A34
- Gaia Collaboration 2024, *A&A*, **686**, L2
- Gosset E., et al., 2025, *A&A*, **693**, A124
- Griffin R. F., 2011, *The Observatory*, **131**, 351
- Griffin R. F., Fekel F. C., 1990, *Journal of Astrophysics and Astronomy*, **11**, 43
- Griffin R. F., Gunn J. E., Zimmerman B. A., Griffin R. E. M., 1985, *AJ*, **90**, 609
- Halbwachs J. L., 1981, *A&AS*, **44**, 47
- Hoffleit D., Warren W. H. J., 1995, *VizieR Online Data Catalog: Bright Star Catalogue, 5th Revised Ed. (Hoffleit+, 1991)*, *VizieR Online Data Catalog: V/50*. Originally published in: 1964BS....C.....0H; 1991bsc..book.....H
- Huang W., Gies D. R., McSwain M. V., 2010, *ApJ*, **722**, 605
- Hulse R. A., Taylor J. H., 1975, *ApJ*, **195**, L51
- Hut P., 1981, *A&A*, **99**, 126
- Jancart S., Jorissen A., Babusiaux C., Pourbaix D., 2005, *A&A*, **442**, 365
- Jayasinghe T., Rowan D. M., Thompson T. A., Kochanek C. S., Stanek K. Z., 2023, *MNRAS*, **521**, 5927
- Jorissen A., Mayor M., 1992, *A&A*, **260**, 115
- Jorissen A., Frankowski A., Famaey B., van Eck S., 2009, *A&A*, **498**, 489
- Katz D., et al., 2023, *A&A*, **674**, A5
- Kervella P., Thévenin F., Lovis C., 2017, *A&A*, **598**, L7
- Kounkel M., et al., 2021, *AJ*, **162**, 184
- Leclerc A., et al., 2023, *A&A*, **672**, A82
- Li S.-s., Li C.-q., Li C.-h., Fan D.-w., Xu Y.-f., Mi L.-y., Cui C.-z., Shi J.-r., 2025, *ApJS*, **276**, 11
- Libert A.-S., 2022, in Celletti A., Galeş C., Beaugé C., Lemaître A., eds, *IAU Symposium Vol. 364, Multi-Scale (Time and Mass) Dynamics of Space Objects*. pp 52–64. doi:10.1017/S1743921321001423
- Loup C., et al., 2019, in Molinaro M., Shortridge K., Pasian F., eds, *Astronomical Society of the Pacific Conference Series Vol. 521, Astronomical Data Analysis Software and Systems XXVI*. p. 50
- Lu W., Rucinski S. M., Ogłóza W., 2001, *AJ*, **122**, 402
- Mahy L., et al., 2022, *A&A*, **664**, A159
- Manchester R. N., Newton L. M., Cooke D. J., Lyne A. G., 1980, *ApJ*, **236**, L25
- Mantelet G., et al., 2023, *Astronomical Data Query Language Version 2.1, IVOA Recommendation 15 December 2023*, doi:10.5479/ADS/bib/2023ivoa.spec.1215M
- Mardling R. A., Aarseth S. J., 2001, *MNRAS*, **321**, 398
- Marrese P. M., Marinoni S., Fabrizio M., Giuffrida G., 2017, *A&A*, **607**, A105
- Marrese P. M., Marinoni S., Fabrizio M., Altavilla G., 2019, *A&A*, **621**, A144
- Mason B. D., Wycoff G. L., Hartkopf W. I., Douglass G. G., Worley C. E., 2001, *AJ*, **122**, 3466
- Matson R., Williams S., Hartkopf W., Mason B., 2006, *Sixth Catalog of Orbits of Visual Binary Stars*. http://www.astro.gsu.edu/wds/orb6.html
- Mazeh T., 2008, in Goupil M. J., Zahn J. P., eds, *EAS Publications Series Vol. 29, EAS Publications Series*. pp 1–65 (arXiv:0801.0134), doi:10.1051/eas:0829001
- McArthur B. E., Benedict G. F., Harrison T. E., van Altena W., 2011, *AJ*, **141**, 172
- Meibom S., Mathieu R. D., 2005, *ApJ*, **620**, 970
- Merle T., 2024, *Bulletin de la Société Royale des Sciences de Liège*, **93**, 170
- Merle T., et al., 2020, *A&A*, **635**, A155
- Merle T., Pourbaix D., Jorissen A., Siopis C., Van Eck S., Van Winckel H., 2024, *A&A*, **684**, A74
- Mirouh G. M., Hendriks D. D., Dykes S., Moe M., Izzard R. G., 2023, *MNRAS*, **524**, 3978
- Moe M., Di Stefano R., 2017, *ApJS*, **230**, 15
- Moore J. H., 1924, *Lick Observatory Bulletin*, **11**, 141
- Moore J. H., 1936, *Lick Observatory Bulletin*, **483**, 1
- Moore J. H., Neubauer F. J., 1948, *Lick Observatory Bulletin*, **521**, 1
- Mowlavi N., et al., 2023, *A&A*, **674**, A16
- Muterspaugh M. W., et al., 2008, *AJ*, **135**, 766
- Muterspaugh M. W., et al., 2010, *AJ*, **140**, 1657
- Osuna P., et al., 2008, *IVOA Astronomical Data Query Language Version 2.00, IVOA Recommendation 30 October 2008* (arXiv:1110.0503), doi:10.5479/ADS/bib/2008ivoa.spec.10300
- Pearce J. A., Hill G., 1975, *Publications of the Dominion Astrophysical Observatory Victoria*, **14**, 319
- Pecaut M. J., Mamajek E. E., 2013, *ApJS*, **208**, 9
- Pourbaix D., 2000, *A&AS*, **145**, 215
- Pourbaix D., et al., 2004, *A&A*, **424**, 727
- Pourbaix D., et al., 2005, *A&A*, **444**, 643
- Pribulla T., Baluďanský D., Dubovský P., Kudzej I., Parimucha Š., Siwak M., Vaňko M., 2008, *MNRAS*, **390**, 798
- Pribulla T., et al., 2020, *MNRAS*, **494**, 178
- Raskin G., et al., 2011, *A&A*, **526**, A69
- Sahlmann J., et al., 2011, *A&A*, **525**, A95
- Sandquist E. L., Latham D. W., Shetrone M. D., Milone A. A. E., 2003, *AJ*, **125**, 810
- Shenar T., et al., 2022, *Nature Astronomy*, **6**, 1085
- Simon M., Obbie R. C., 2009, *AJ*, **137**, 3442
- Spencer Jones H., 1928, *Annals of the Cape Observatory*, **10**, 8
- Stokes G. H., Taylor J. H., Dewey R. J., 1985, *ApJ*, **294**, L21
- Struve F. G. W., 1827, *Catalogus Novus Stellarum Duplicium et Multiplicium: maxima ex parte in specula Universitatis Caesarea Dorpatensis per magnum telescopium achromaticum Fraunhoferi detectarum*
- Tan J., Lewin W. H. G., Hjellming R. M., Penninx W., van Paradijs J., van der Klis M., Mitsuda K., 1992, *ApJ*, **385**, 314
- Thorstensen J. R., Patterson J., Kemp J., Vennes S., 2002, *PASP*, **114**, 1108
- Tokovinin A., 2018, *ApJS*, **235**, 6
- Tokovinin A., 2020, *AJ*, **160**, 69
- Tokovinin A., 2022, *AJ*, **163**, 161
- Tokovinin A., 2023, *AJ*, **165**, 220
- Tokovinin A. A., Gorynya N. A., 2001, *A&A*, **374**, 227
- Tokovinin A., Latham D. W., 2020, *AJ*, **160**, 251
- Tokovinin A., Thomas S., Sterzik M., Udry S., 2006, *A&A*, **450**, 681
- Tokovinin A., Mason B. D., Mendez R. A., Costa E., 2022, *AJ*, **164**, 58
- Tomkin J., 2003, *The Observatory*, **123**, 1
- Torres G., 2006, *AJ*, **131**, 1702
- Torres G., Stefanik R. P., 2000, *AJ*, **119**, 1914
- Tsantaki M., et al., 2022, *A&A*, **659**, A95
- Udry S., Jorissen A., Mayor M., Van Eck S., 1998, *A&AS*, **131**, 25
- Van Den Berg M., Orosz J., Verbunt F., Stassun K., 2001, *A&A*, **375**, 375
- Videla M., Mendez R. A., Clavería R. M., Silva J. F., Orchard M. E., 2022, *AJ*, **163**, 220
- Wellmann H., Wellmann P., 1960, *Z. Astrophys.*, **49**, 206
- Wenger M., et al., 2000, *A&AS*, **143**, 9
- Winn J. N., Fabrycky D. C., 2015, *ARA&A*, **53**, 409
- Yavuz İ., 1968, PhD thesis, University of Hamburg, Germany
- Zasche P., et al., 2019, *A&A*, **630**, A128
- van Kerkwijk M. H., Kulkarni S. R., 1999, *ApJ*, **516**, L25
- van Leeuwen F., 2007, *A&A*, **474**, 653

APPENDIX A: S_{B9} DISTRIBUTIONS FOR DWARF AND GIANT COMPONENTS

APPENDIX B: CROSS-MATCH STRATEGY

Before performing the cross-match, we first uploaded the S_{B9} catalogue from external TAP (CDS VizieR) to the *Gaia* archive (in Advanced ADQL tab). Then, we used the query:

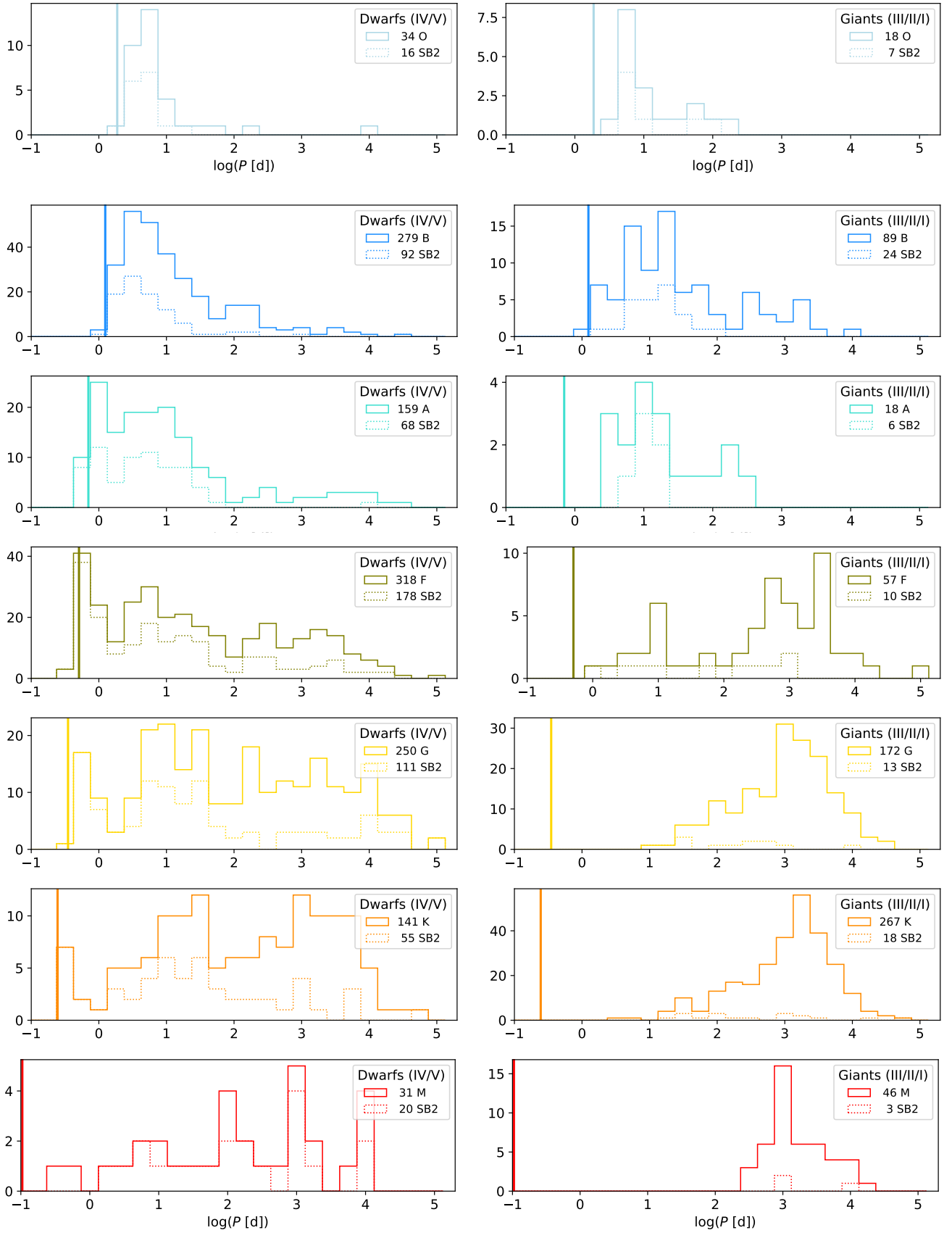


Figure A1. Distribution, in absolute numbers, of the S_{B9} orbital periods per spectral type for dwarfs, corresponding to luminosity classes of IV and V (left) and for giants, corresponding to luminosity classes of III, II and I (right) for the SB primary component. Colour codes spectral type. Vertical lines correspond to the minimum period estimated for a contact equal-mass binary of a given spectral type.

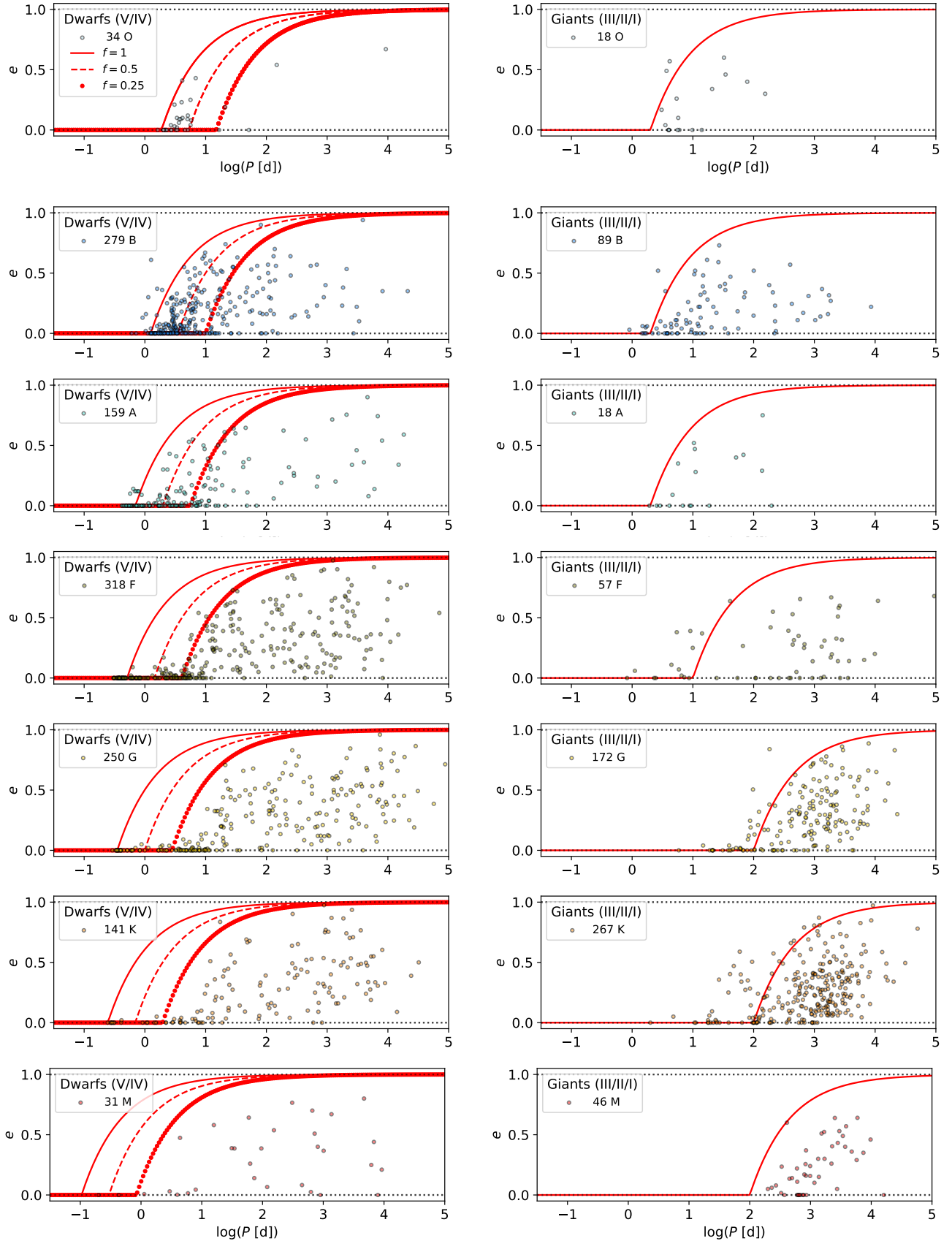


Figure A2. Eccentricity-period diagrams of S_{B9} binaries per spectral type for dwarfs, corresponding to luminosity classes V and IV (left) and for giants, corresponding to luminosity classes III, II and I (right) for the SB primary component. Colour codes spectral type. *Periastron* envelopes for three different values of the filling factor f and their corresponding circularisation periods are displayed (Eq. 2 and Table 1) for main sequence primaries (left panels). For giant primaries, $f = 1$ *periastron* envelopes are displayed for $P_c = 2$ d (OBA giants), $P_c = 10$ d (F giants), and $P_c = 100$ d for GKM giants.

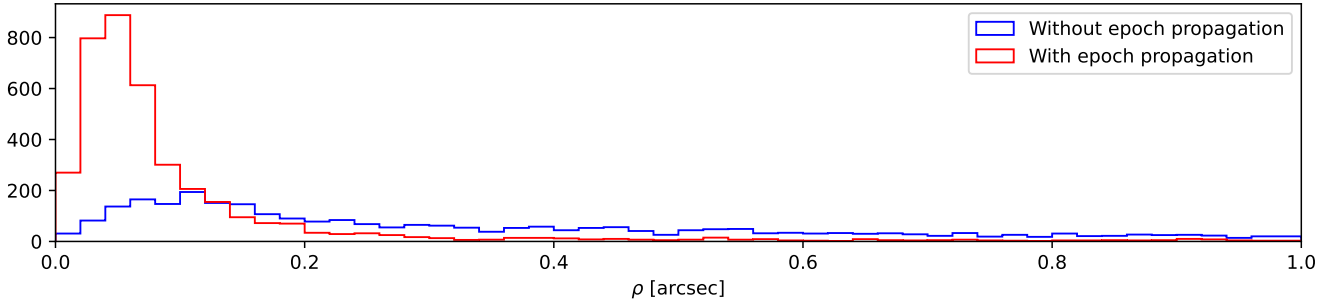


Figure B1. Cross-matched angular separation between S_{B9} and *Gaia* with (red) and without (blue) epoch propagation. The median angular separation is 0.24 arcsec without back propagation of the *Gaia* epoch, and it is reduced to 0.06 arcsec with epoch propagation.

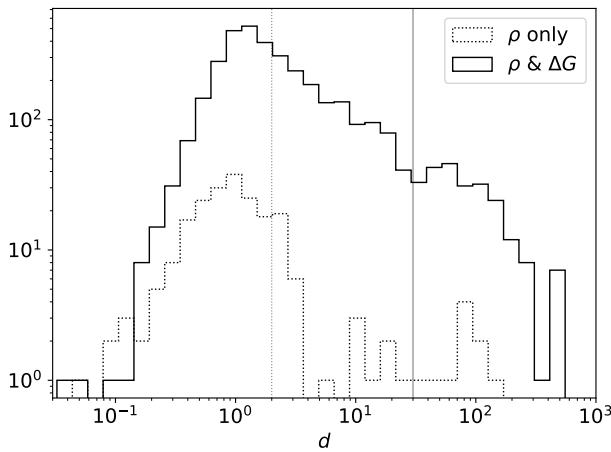


Figure B2. Distribution of Euclidean distances for one-to-one and one-to-many ‘best’ matches, corresponding to 3712 systems. We manually check all systems with $d > 2$ when only separation match ρ is available; and with $d > 30$ when both separation match and magnitudes difference ΔG are available.

```
SELECT *
FROM "B/sb9/main"
WHERE Seq <= 4021
ORDER BY Seq
```

where the condition on Seq is done to select the 2021-03-02 version of the catalogue. We reiterate this query for "B/SB9/orbits" and "B/SB9/alias". We thus obtain 4021 systems and 5042 orbits as expected. From the resulting queries, we create user tables to allow ADQL queries from both *Gaia* and S_{B9} catalogues. The S_{B9} coordinates from VizieR are claimed to be in the FK5 system, and are computed by VizieR¹⁵. The difference between the FK5 (equinox J2000.0) and the ICRS systems is of the order of 50 mas (Feissel & Mignard 1998), which is much larger than the *Gaia* DR3 median position uncertainties of 0.05 mas at $G < 17$ (magnitudes in S_{B9} reach $G = 19$), but remains reasonably low compared to the size of the cone search radius used in the cross-match.

Prior to the cross-match, we select a first subset of *Gaia* DR3 sources around the S_{B9} coordinates with a cone search radius of 170 arcsec. Indeed, the displacement over 16 years of the Barnard’s star, the star with the highest proper motion (Barnard 1916), is 166.133 arcsec, computed by retro-

propagating its position from epoch J2016 to J2000. With such a large cone, we obtain a subset of more than 1.8 million *Gaia* matches, no limits on magnitude being imposed. The advantage of this method allows to compute the back-propagation only for this subset. We make the epoch back-propagation with the ADQL function EPOCH_PROP_POS which relies on the 6 astrometric parameters (right ascension, declination, parallax, the two proper motions and the radial velocity) from the *Gaia* DR3 epoch (J2016.0) to the S_{B9} epoch (J2000.0). We note that the ADQL function, while returning right ascension, declination, parallax and the two proper motions in the same units as the function inputs, does return the propagated radial velocity¹⁶ in mas a^{-1} and not in km s^{-1} ; the returned quantity needs to be multiplied by A/ϖ , where A is the astronomical unit ($A = 4.740470446 \text{ km s}^{-1} \text{ a}$) and ϖ the parallax in mas, to obtain the radial velocity in km s^{-1} , as explained in the *Gaia* DR3 documentation¹⁷.

Finally we performed the cross-match at epoch J2000.0 with a cone search radius of 10 arcsec. We obtain at least one cross-match pair for 3981 out of the 4021 S_{B9} systems and 8710 unique *Gaia* sources. Thanks to the epoch back-propagation, we recovered 26 S_{B9} systems. In addition, the histograms of Fig. B1 shows that the median of the cross-match separation ρ is decreased by a factor of four (from 0.24 to 0.06 arcsec) when epoch propagation is considered. With this strategy, there were some S_{B9} systems without a *Gaia* match within 10 arcsec. Among them, we identified 21 S_{B9} systems without a match in *Gaia* DR3 because they are brighter than $G = 3$ (see Table 2). These include many of the brightest binaries in their constellations, such as α Cen, Sirius, Procyon; triple systems like Algol; and even higher-order systems such as Capella (α Aur) and Castor A and B (α Gem). At the opposite end, there are six S_{B9} systems that are too faint to be observed by *Gaia* (see Table 3). They include a low-mass X-ray binary, UY Vol (Crampton et al. 1986), a binary with a pulsar, PSR J0823+0159 (Manchester et al. 1980) and two faint SB identified in SDSS (Pourbaix et al. 2005). At later stages, we also add the Hulse-Taylor binary pulsar (Hulse & Taylor 1975) and PSR J2305+4707 (Stokes et al. 1985).

A basic search¹⁸ in the *Gaia* archive for the three remaining systems without *Gaia* matches revealed that the angular separation was larger than the 10 arcsec threshold chosen (S_{B9} 562, 2098 and 2454 with approximately, 16, 11 and 42 arcsec). The treatment of these cases is performed separately and manually.

APPENDIX C: BEST MATCH SANITY CHECKS

For each S_{B9} system, we select as ‘best’ match the one with the lowest Euclidean distance. We display the distribution of these Euclidean distances

¹⁶ It is actually the proper motion in the radial direction which is computed by the EPOCH_PROP_POS ADQL function.

¹⁷ 3.1.7 Transformations of astrometric data and error propagation

¹⁸ Based on the Sesame resolver from SIMBAD (Wenger et al. 2000).

¹⁵ <https://cdsarc.cds.unistra.fr/viz-bin/cat/B/sb9>

Table D1. 18 S_{B9} system duplicates sorted per original system number.

duplicate number	S_{B9} system number	Name
2544	374 ¹	μ Ori AB
2169	376 ²	64 Ori
3779	1568	HD 196673A
2917	1981	NGC 3960 50
2904	2359	NGC 2489 25
2927	2364	NGC 5822 312
2897	2489	BD –14 2111
2938	2484	NGC 6940 111
2939	2485	NGC 6940 130
2890	2487	NGC 2360 51
2893	2488	BD –15 1742
2923	2491	NGC 5822 11
2928	2494	NGC 5823 34
2875	2498	NGC 2099 149
2877	2503	HD 248448
2878	2506	NGC 2099 966
2879	2507	NGC 2099 1505
2902	2530	NGC 2477 430

¹ Member of a spectroscopic quadruple with S_{B9} 372 (SB1) and 373 (SB2); see Table 4.

² Member of a spectroscopic triple with S_{B9} 375.

in Fig. B2. We performed a manual check of *oto* and *otm* matches with the largest Euclidean distances. For the 245 S_{B9} systems without magnitude (6%), the Euclidean distance only relies on the angular separation. For those, we manually check all the best matches with Euclidean distance $d > 2$ corresponding to 40 system numbers. Among them we identify 3 S_{B9} systems with erroneous ‘best’ matches. For all the other systems with ρ and ΔG available, we investigated all the *oto* and *otm* systems with $d > 30$, which concern 232 system numbers ($\sim 6\%$). Many of them are cataclysmic binaries, classical novae, symbiotic stars, hot subdwarfs, white dwarfs, etc. showing a large photometric discrepancy between *Gaia* and S_{B9} . Among them, we identify 26 S_{B9} systems with erroneous ‘best’ *oto* and *otm* matches. For instance S_{B9} 1503 has wrongly been attributed the coordinates of HD 895, a Tycho visual binary (Fabricius et al. 2002), while it actually is HD 895 C, a close SB2, making the overall system at least a quadruple.

We also performed a manual check of all best matches that involve two or more S_{B9} systems per *Gaia* source (corresponding to *mto* and *mtm* matches). This involves inspecting the best matches attached to 124 unique *Gaia* sources, corresponding to 253 unique S_{B9} system numbers. It reveals the presence of many SB belonging to high-order systems (Sec. 3.2.3.1) as well as some duplicates (Sec. 3.2.3.2).

APPENDIX D: S_{B9} SYSTEM DUPLICATES

APPENDIX E: TRIPLE SYSTEMS WITH ORBITS IN S_{B9}

APPENDIX F: QUADRUPLE SYSTEMS WITH ORBITS IN S_{B9}

APPENDIX G: HIGH-ORDER SYSTEMS WITH ORBITS IN S_{B9}

APPENDIX H: THE COMMON SAMPLE $S_{B9} \cap \text{NSS}$

This paper has been typeset from a $\text{\TeX}/\text{\LaTeX}$ file prepared by the author.

Table E1. List of 76 triple systems with S_{B9} orbits.

S_{B9}	<i>Gaia</i>	SIMBAD	in NSS	Separation [arcsec]
27, 2545	2528433919872925312	* 13 Cet		
49, 1726	426512590631144704	HD 5408		
122, 123	457464770661735296	V* DM Per		
157, 158	too bright	* bet Per		
169, 2464	118986060277836160	V* UX Ari		
211, 212	3305012316783533056	* lam Tau		
226, 227	270632490692926720	* b Per		
262, 1629	3313241714640886400	HD 285947		
319, 320	3214077516844988800	* eta Ori A		
332, 333	3217626018825418752	V* VV Ori		
375, 376	3374718330328109440	* 64 Ori		
430, 431	3046036062400216576	V* FZ CMa		
490*, 3941	654808519221768192	V* UU Cnc	EB	
609, 2617	5668792270155162240	V* HS Hya		
718, 1727	3695061317957036928	* eta Vir		
733*, 3874	3962579368940811904	HD 110195	SB2	
789, 790	6293889335197400064	V* DL Vir		
817, 818	1241620894326361344	HD 129132		
828, 2993	1391924687894823296	V* TZ Boo		
856, 2386	1374695306328813568	* 7 CrB A		
962, 963	4490117076492339712	HD 157978		
1023, 1024	4576326312902814208	HD 165590A, HD 165590		
1028, 2463	4590455518346609792	HD 166181		
1055, 1056	4273231054929181824	* d Ser A		
1134, 1135	6770084041623596032	* psi Sgr		
1172, 2142	2031776202613700480	V* SU Cyg		
1223, 1224	6875990375999580544	* bet02 Cap, * bet01 Cap		
1253, 3632	1735416587180214528	HD 196795 A, HD 196795		
1280, 2460	1873073175244118784	BD+40 883 A, BD+40 883		
1288, 1289	1852355455594429440	HD 201433A		
1293, 1294	2191133748536265216	HD 203025		
1296, 1297	1745244296985069184	HD 203345		
1319, 1320	1741318868675197184	V* EE Peg		
1390, 1391	1982245024789617280	HD 214608		
1431, 1432	2658510028089009792	HD 219018		
1493, 1494	4472789731012285824	BD+04 35622		
1508, 3080	2231007778225666944	HD 214511		
1595, 1596	368060765779919360	BD+38 118		
1624, 1625*	1070770191963666816	HD 83270	AB	
1659, 1660*	992435451683384320	V* V455 Aur	SB2	
1723, 1724	1683524861026802176	HD 105287		
1729, 1730	1746335802793081344	HD 202908		
1731, 1732	1346932740806216960	V* V819 Her		
1752, 1753	1652148132065326720,	HD 158209		
1769, 1770	5350358069101053184	V* V572 Car		
1815, 1834	604921542069455104, 604921546365012480	NGC 2682 131, NGC 2682 131 A		0.4
1835, 1836	6731200706257840384	V* TY CrA		
1919, 1977	664288577196528128	HD 73174		
2408, 2409	2768404669096691072	V* LN Peg		
2411, 2412	3582095053777917952	V* HU Vir		
2456, 2458	1975001785790477312	V* SS Lac	SB2	
2477, 2906	5727490488683081216	BD-12 2381		
2561, 2592	2791062373929675904	HD 7119	SB2	
2562, 2591	859117605230828032	AG+59 808		
2588, 2594	2058736124602103552	HD 191588		
2602, 2603	5452239641134855168	HD 97131		
2604*, 2605	1518695423639372160	HD 109648	SB2	
2606, 2607	2169527108088349952	V* V1061 Cyg		
2682, 3927	4031448894654813696	HD 103613		
2683, 2684	4339465085630200960	HD 152751		
2754, 2755	478368788803049600	HD 32893		
2806, 2807	3916285149112698240	HD 100518 A		
3449*, 3450	661306319407420160	BD+19 2077	SB2	
3500, 3501	3465682748358563968	HD 104471 A, HD 104471		
3518, 3519	4618008180223988352	HD 10800		
3520, 3521	4755117967402573056	HD 18198 A, HD 18198		
3522, 3523	4614931093854496640	HD 35877		
3552*, 3805	3378123861436589952	HD 48565	SB1	
3615, 3616	458319228639270016	HD 14039		
3699, 3700	6898265656937739648	HD 204236		
3701, 3702	2619653390242676096	HD 211276		
3727, 3728	464891250151058816	BD+60 585	AB	
3870, 3871	1517909994379553152	HD 109803		
3872, 3873	3959246783557460096	HD 109954		
3966, 3967*	242935724068826368	HD 20577	SB1	
4016, 4017	2653803053170408832	HD 214169		

Notes. *Gaia* DR3 separations are computed at epoch J2016.0. An asterisk (*) indicates membership in the clean common sample.

Table F1. List of the 34 quadruple systems with S_{B9} orbits including two probable optical quadruples.

S_{B9}	<i>Gaia</i>	SIMBAD	in NSS	Separation [arcsec]
87, 1504	292304861302115072, 292304861302114816	HD 10308, HD 10308 B		10.3
112, 113	300312157810876544, 300312157810876160	* iot Tri A, * iot Tri B		3.9
181, 1523	3263936692671872384, 3263936658312134272	HD 22468, HD 22468 B		6.7
216*, 2052	476270508301993344	HD 25638	EB	
372, 373, 374	3329650894896257024	* mu. Ori A, * mu. Ori B, * mu. Ori		
461, 462	too bright	* alf Gem B, * alf Gem A		
514, 515	3072894691921171456	HD 71663		
532, 533	583151353574583552, 583151353574583424	* eps Hya, * eps Hya C		2.8
575, 1506	813111839701758080, 813111835405980928	* A Hya, AG+40 1074		25.0
593, 594	623076270045202048	V* XY Leo		
1948, 635	5350346970905044480, 5350346970887961984	HD 93206, HD 93206 B		1.0
667, 668	756853643637996160, 756853643638639104	* ksi UMa B, * ksi UMa A		1.8
734, 735	3528976341368900096, 3528976341368899712	V* VV Crv, HD 110318		5.2
764, 765	1563590579347125632, 1563590510627624064	* zet01 UMa, * zet02 UMa		14.4
858, 859	1217683254878932352	HD 140629A, HD 140629 B		
885, 2403	4456633958128648832	HD 144515		
1524, 1525	150461092453290240	* chi Tau B		
1559, 1607	97746175687968768, 97746137032809984	BD+21 255, TYC 1212-473-1	-, SB	53.5 (optical?)
1747, 1748	3115721215281475840, 3115721219581645952	BD+02 1483 A, BD+02 1483 B		0.9
1773, 1774	5350357862947802880	CPD-59 2636		
1838, 1844	401249764784080000, 401249764784080384	HD 6645, HD 6645 B		8.7
2394, 2461	4661730461966674304	SK -67 18		
2415, 2416	2869876947957928576	HD 221264		
2449, 2450	3534414590303807232, 3534414594600352896	HD 98800 A, HD 98800 B		0.5
2620*, 2621	3365396498949922432	HD 49635	AB	
2700, 2701	389688601879413248, 389688606176165248	HD 4134 A, HD 4134 B		
2984, 3210	1587395899441029760	V* ET Boo		
2985, 3214	1700166038233698048	HD 133767		
2989, 2994	4175947159460432384	HD 162905		
3213, 4003, 4004	733549185449902208	HD 95660		
3539, 3540	3708802460231857664, 3708802464524486656	HD 110555 A, HD 110555 B		0.6
3649, 3650	294090502544836992, 294090536905167744	* phi Psc B, * phi Psc		7.6
3839, 3840	2155746340444188544, 2155746413460589696	HD 179332, BD+60 1892	AB, -	47.8 (optical?)
3875, 3876, 3877	1441569596393755648	HD 117078		

Notes. *Gaia* DR3 separations are computed at epoch J2016.0. An asterisk (*) indicates inclusion in the clean common sample.

Table G1. List of the six higher-order multiple systems with S_{B9} orbits.

S_{B9}	<i>Gaia</i>	SIMBAD	in NSS	Separation [arcsec]	MSC
257, 1527	3293714285052444800, 3293714491209540352	* 88 Tau, * 88 Tau B	-, AB	69.5	sextuple
305, 1484	180702438220217344, 180702438220219904	* 14 Aur, * 14 Aur B		14.2	quintuple
340, 341	3017364132050194688, 3017364132049943680	* tet01 Ori A, * tet01 Ori B		8.9	Orion Trapezium
461, 462, 463	too bright, too bright, 892348454394856064	* alf Gem B, * alf Gem A, V* YY Gem			sextuple
1510, 1511	1374656960860690560, 1374656960861310336	HD 139691 A, NAME AG+36 1364 B		15.0	sextuple
1023, 1024, 1986	4576326312902814208, 4576326312902814208, 4576326312901650560	HD 165590 A, HD 165590, V* V885 Her		28.5	quintuple

Table H1. The common sample of 827 binaries between S_{B9} and *Gaia* DR3 NSS.

sb9	gaia	simbad	outlier	in_triple	in_quadruple	in_hom	nss_solution_type	family
11	4924503334299333888	HD 1273	False	False	False	False	SB1	
13	4689821167286415744	V* AQ Tuc	False	False	False	False	EclipsingBinary	
15	428246623544412416	V* TV Cas	False	False	False	False	EclipsingBinary	
16	2857501394830370944	V* LR And	False	False	False	False	SB1	
18	2862259565759107200	HD 2019	True	False	False	False	SB2	
...								
216	476270508301993344	HD 25638	False	False	True	False	EclipsingBinary	(216, 2052)
...								
490	654808519221768192	V* UU Cnc	False	True	False	False	EclipsingBinary	(490, 3941)
...								
1527	3293714491209540352	* 88 Tau B	True	False	False	True	Orbital	(257, 1527)

Notes. The column definitions are as follows: sb9 is the S_{B9} identifier, gaia is the *Gaia* DR3 source_id, simbad is the main SIMBAD identifier. outlier is true if the relative-period or absolute-eccentricity difference exceeds 10in_triple, in_quadruple, and in_hom flag multiplicity categories. nss_solution_type follows the DR3 Non-Single Star schema. The clean common sample corresponds to outlier = False and contains 655 systems.